ESCOLA
SUPERIOR
DE SAÚDE
POLITÉCNICO
DO PORTO

M

MESTRADO BIOQUÍMICA EM SAÚDE
RAMO DE CLÍNICA E METABÓLICA

ADP-ribosylation of host cell proteins in *Salmonella* infection

Rita Pinto

12/2018

Escola Superior de Saúde

Instituto Politécnico do Porto

ADP-ribosylation of host cell proteins in *Salmonella* infection

Rita Pinto

Mestrado em Bioquímica em Saúde

Ramo de Clínica e Metabólica

Dezembro 2018

Escola Superior de Saúde

Instituto Politécnico do Porto

Rita Pinto

Dissertation submitted to School of Health of Porto to fulfil the necessary requirements to obtain the Master's degree in Biochemistry in Health, accomplished under scientific guidance of Arto Pulliainen, PhD, Adjunct professor at University of Turku and Moona Miettinen, PhD student of University of Turku, Finland and institutional guidance of Arto Pulliainen, PhD, Adjunct professor at University of Turk and Cristina Prudêncio, MD, PhD, from the Department of Chemical Sciences and Biomolecules of the School of Health of Porto, Portugal.

Dissertação submetida à Escola Superior de Saúde do Porto para cumprimento dos requisitos necessários à obtenção do grau de Mestre em Bioquímica em Saúde, realizada sob a orientação científica de Moona Miettinen, aluna de Doutoramento da Universidade de Turku, Finlândia, e orientação institucional de Doutor Arto Pulliainen, Professor adjunto da Universidade de Turku e da Professora Doutora com Agregação Cristina Prudêncio, Departamento de Ciências Químicas e das Biomoléculas da Escola Superior de Saúde do Porto, Portugal.

Dezembro 2018

Acknowledgments

Em primeiro lugar, quero agradecer à Escola Superior de Saúde por esta oportunidade e a todos os meus professores que me ajudaram a chegar aqui.

To Doctor Arto Pullianen, the biggest appreciation in the world for giving a chance to this southern European. Thank you for all teachings and inspiration shared. I would also like to thank all my work colleagues for creating such a wonderful and welcoming atmosphere and special thanks to Moona for the everlasting patience to my never-ending and untimely questions.

Aos meus colegas de mestrado, um grande obrigado nesta etapa da minha vida. Está feito!

Aos meus amigos, desculpem o sumiço. Vou recompensar-vos por não terem desistido em mim. Ana Rita, minha quarta orientadora, obrigada, sem ti não sei se teria acabado isto.

Por último e mais importante, quero agradecer à minha incrível família. Obrigada por toda a paciência com as minhas crises existenciais, o apoio, apesar de nada de isto vos fazer sentido, e por me manterem no mundo macroscópico invés do microscópico.

Financial support mention

I would like to thank the Erasmus programme for allowing me this opportunity as well as for the support given.

The research in the laboratory of Dr. Arto Pulliainen is financially supported by Academy of Finland (Academy Project, No 295296, 2016 – 2020), Sigrid Jusélius Foundation (Junior group leader grant, 2015 – 2018) and University of Turku, Turku, Finland.

Summary

ADP-ribosylation is a reversible enzymatic post-translational modification consisting in the transfer of one or many ADP-ribose residues from NAD^+ to a target protein. ADP-ribosylation signalling has been linked to cancer and immune responses. Many bacterial protein toxins have been identified to act through ADP-ribosylation of protein targets inside the host cell. This project is based on a hypothesis that endogenous host cell poly-(ADP-ribose) polymerases (PARPs) become activated in bacterial infection and ADP-ribosylate specific host cell proteins to influence pathogen clearance.

Mono- and poly-(ADP-ribose)-specific Western blotting was first used to detect ADP-ribosylated proteins during *Salmonella* infection and lipopolysaccharide (LPS) or cytokine stimulation of different cell types. Multiple ADP-ribosylated proteins originating either from host cell or the invading *Salmonella* was detected. It was found that, similarly to *Salmonella* infection, LPS induced ADP-ribosylation of the host cell proteins. Cytokines did not induce ADP-ribosylation of the host cell proteins. Macrophages displayed more robust changes in ADP-ribosylated proteins as compared to epithelial cells. Secondly, quantitative PCR and Western blotting were used to quantify expression levels of PARPs during *Salmonella* infection and LPS or cytokine stimulation of different cell types. It was detected one protein to be mono-ADP-ribosylated in both epithelial cells and macrophages. Macrophages showed two additional signals identified as poly-ADP-ribosylation. LPS stimuli in macrophages showed proteins poly-ADP-ribosylated at similar size of one found in bacterial infection. Cytokines did not induce ADP-ribosylation in macrophages. In epithelial cells both LPS and cytokines showed to increase expression of PARP1, while *Salmonella* had no effect in its expression, whereas in macrophages, PARP1 had different expression by stimuli of bacteria and cytokines but LPS had no effect. As for PARP14 expression in epithelial cells, LPS and TNFα had no effect in its expression however, it showed changes in expression when incubated with the interferons and *Salmonella*. In macrophages, TNFα remained to have no effect in PARP14 expression while all the other caused differential expression of the enzyme. Lastly, stimulation with bacteria or LPS and IFNγ led to changes in expression values of *parp1* and *parp14*.

In conclusion, endogenous host cell PARPs become upregulated, activated and ADP-ribosylated host cell proteins in *Salmonella* infection. These changes might benefit the invading bacterium or the human host cells. The results provide the basis for future

experimentation on the importance of PARPs and ADP-ribosylation in bacterial infection. This knowledge may allow the development of targeted therapeutic strategies for emerging antibiotic resistant bacteria, potentially involving PARP targeting.

Key words: ADP-ribosylation, poly-(ADP-ribose) polymerases, *Salmonella*, cytokine, inflammation

Resumo

ADP-ribosilação é uma modificação enzimática pós-tradução, consistindo na transferência de um ou mais resíduos de ADP-ribose de NAD^+ para a proteína alvo. A sinalização de ADP-ribosilação foi relacionada a cancro e respostas imunes. Muitas toxinas bacterianas proteicas foram identificadas a actuar através da ADP-ribosilação de alvos proteicos dentro da célula alvo. Este projecto é baseado na hipótese que poli-(ADP-ribose) polimerases endógenas à célula hospedeira activam-se em infecções bacterianas e ADP-ribosilam proteínas especificas na célula hospedeira para influenciar a *clearance* patogénica.

Western blotting específico para mono- e poli-(ADP-ribose) foi inicialmente usado para detectar proteínas ADP-ribosiladas durante uma infecção por salmonela e estimulação por lipopolisacarídeo (LPS) ou citocinas em diferentes tipos de células. Foram detectadas múltiplas proteínas ADP-ribosiladas originadas pela célula hospedeira ou da *Salmonella* invasora. Observou-se que, semelhante à infecção por *Salmonella*, LPS também induzia ADP-ribosilação de proteínas da célula hospedeira. Citocinas não induziram ADP-ribosilação na célula hospedeira. Macrófagos demonstram mudanças mais robustas em proteínas ADP-ribosiladas quando comparadas com células epiteliais. Segundamente, PCR quantitativo e Western blotting foram usados para quantificar os níveis de expressão de PARPs durante infecção por *Salmonella* e estimulação por LPS ou citocinas em diferentes tipos de células. Foi detectada uma proteína mono-ADP-ribosilada em células epiteliais e macrófagos. Em macrófagos foram visualizados dois sinais adicionais identificados como poli-ADP-ribosilação. Estímulo por LPS em macrófagos demonstrou uma proteína poli-ADP-ribosilada com tamanho semelhante à encontrada em infecção bacteriana. Citocinas não induziram ADP-ribosilação em macrófagos. Em células epiteliais, tanto LPS como citocinas demonstraram expressão diferenciada de PARP1, enquanto nenhum efeito foi detectado por *Salmonella*. Por sua vez, em macrófagos, PARP1 demonstrou uma expressão alterada por estímulo de bactérias e citocinas, mas LPS não demonstrou efeito. Em relação à expressão de PARP14, em células epiteliais, LPS e TNFα não demonstraram qualquer efeito, mas, no entanto, demonstrou mudanças na sua expressão quando incubado com os interferões e *Salmonella*. Em macrófagos, TNFα continuou a não ter efeito na expressão de PARP14 enquanto outras citocinas, LPS e *Salmonella* causaram expressão diferenciada da enzima. Por último, estimulação por bactérias ou LPS e IFNγ levou a mudanças nos valores de expressão de *parp1* e *parp14*.

Concluindo, PARPs endógenas à célula hospedeira tornam-se sobre reguladas, activadas e ADP-ribosilam proteínas da célula hospedeira em infecção por *Salmonella*. Estas alterações podem beneficiar as bactérias invasoras ou as células hospedeiras humanas. Os resultados providenciam bases para futura experimentação na importância de PARPs e ADP-ribosilação em infecção bacteriana. Este conhecimento poderá permitir o desenvolvimento de estratégias terapêuticas direccionadas para bactérias resistentes a antibióticos emergentes, potencialmente intencionadas para PARP.

Palavras chave: ADP-ribosilação, poli-(ADP-ribose) polimerases, *Salmonella*, citocinas inflamação

Index

Abbreviations

ADP, adenosine diphosphate; ARH, ADP-ribose hydrolase; ART, ADP-ribose transferase; ARBD, ADP-ribose binding domains; ARTCs, ADP-ribose transferases cholera toxin-like; ARTDs, ADP-ribose transferases diphtheria toxin-like; DMEM, Dulbecco's modified eagle medium; DNA, deoxyribonucleic acid; DSB, double-stranded breaks; FBS, fetal bovine serum; GAPDH, Glyceraldehyde-3-phosphate dehydrogenase; GFP, green fluorescent protein; GST, glutathione S-transferase; HRP, horseradish peroxidase; HSV, herpes simplex virus; ICAM, intercellular adhesion molecule 1; IFN, interferon; LPS, lipopolysaccharide; MAR, mono-ADP-ribose; MARTs, mono-ADP-ribosylating transferases; mRNA, messenger RNA; NA, nicotinic acid; Nam, nicotinamide; NAD+, nicotinamide adenine dinucleotide; NAMPT, nicotinamide phosphoribosyltransferase; OD, optimal density; PAR, poly-ADP-ribose; PARG, poly-ADP-ribose glycohydrolase; PARP, poly-ADP-ribose polymerase; PBM, PAR-binding motifs; PBZ, PAR-binding zinc finger; PMA, phorbol myristate acetate; PTM, post-translational modification; qPCR, quantitative polymerase reaction chain; RNA, ribonucleic acid; RPMI, Roswell Park Memorial Institute 1640 medium; Sop, *Salmonella* outer proteins; SPI, *Salmonella* pathogenicity island I; *Spv*, *Salmonella* plasmid virulence; SSB, single-stranded breaks; T3SS, type 3 secretion system; TNF, tumor necrosis factor.

Other indexes

Figures index

Introduction

Antibiotic resistant bacteria are a very current problem with incidence of infections on the rise. Antibiotics are getting out-dated faster than they are being created and there is a need to find new ways to fight bacteria. Identifying the pathways thru which bacteria infect can lead to new ways to the development of mechanisms to fight such bacteria.

Post-translational modifications (PTM) come as one way to establish homeostasis within the cell as modifications in certain amino acids affect their activity, whether they are needed or, by opposition, when their use has been spent. PTMs play a role in the survival of the cells as well as in their growth and reproduction. PTMS are used by both bacteria and host cell for one to subdue the other. ADP-ribosylation is one of the more than 300 PTM exerted by the cells and one highly conserved. Present in all kingdom of life it is found to have full functions in microbial pathogenicity as well as in DNA damage repair in more complex organisms.

As new ways to fight infection are in need and therapies targeting endogenous ADP-ribosylation are already in use for cancer, perhaps the development of this therapies for bacterial infection could present a novel option for the improvement of antibiotics.

The work present in this dissertation aims to elucidate on the endogenous ADP-ribosylation function of the host cell and thenceforth gain insight in the multitude of events that make up the infections.

Chapter I – Bibliographic review

1. ADP-ribosylation

ADP-ribosylation is a reversible post-translational modification (PTM) consisting in the transfer of ADP-ribose from NAD^+ to the target protein. It was first identified in the diphtheria toxin as mechanism underling its pathogenicity in 1964 (Aravind, Zhang, de Souza, Anand, & Iyer, 2014). Since then, it has been recognized in other bacteria, eukaryotes and virus and even to be involved in cell functions as DNA damage, cell survival and cell death as well as host-virus interactions and cellular stress responses (Gupte, Liu, & Kraus, 2017). As consequence of ADP-ribosylation, target proteins activity is altered, so as their binding partners and it can even be targeted for degradation by ubiquitination. Not only do proteins serve as target, nucleic acids and antibiotics can also be ADP-ribosylated (Hottiger, Hassa, Lüscher, Schüler, & Koch-Nolte, 2010).

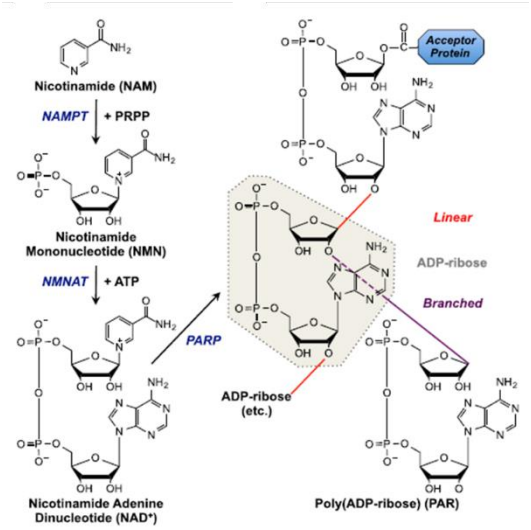

Figure 1 – Representation of synthesis of NAD^+ from Nicotinamide and ADP-ribosylation with formation of both poly(ADP-ribose) and mono(ADP-ribose) (Kraus, 2015).

ADP-ribosylation is an ancient PTM catalysed by a family of enzymes called ADP-ribosyltransferases (ARTs)(Palazzo, Mikoč, & Ahel, 2017). ARTs are an example of an evolutionary fight between pathogen and host due to structural similarities between bacterial and eukaryotic ARTs. ADP-ribosylation by ARTs can occur as mono-ADP-ribosylation (MARylation) when it is only one unit of ADP-ribose or as poly-ADP-ribosylation (PARylation) when a polymer of ADP-ribose is added to the substrate (Aravind et al., 2014).

MAR is thought to be originated as a defence mechanism from bacteria against viruses. But as we go from prokaryotic cells to multicellular eukaryotes the complexity of the ARTs evolves in substrates specificities, sequence and structure. Human ARTs are larger, more complex and more diverse in terms of non-catalytical domains than the bacterial ARTs (Aravind et al., 2014). PARylation has, in fact, only been identified in eukaryotic cells (Hottiger et al., 2010).

The ARTs are classified according to the structure of the catalytic domain, substrate specificity, type of ADP-ribosylation (mono-, oligo- or poly-) and the nature of the covalent bond. As subclasses they are divided between the diphtheria-like toxins (ARTDs) and cholera-like toxins (ARTCs) whereas as families they are divided between mono-ADP-ribosyltransferases (MARTs), poly-ADP-ribosyltransferases (PARPs). So far it has been identified Cysteine, Glutamate, Serine, Diphthamide, Asparagine, Arginine and Lysine as substrates with the target proteins (Hottiger et al., 2010).

The ART fold characterized by being structurally well conserved but at the sequence level it is poorly conserved within in all ART family members (Aravind et al., 2014). This core is composed of a β-sheet made of 6 strands. Within this core there are 3 motifs found to be conserved in all the ARTs distributed among the first, second and between the fifth and the ADP-ribosylating turn-turn loop. Both the first and second motif are involved in the NAD^+-binding. The second motif found as Serine-Threonine-Serine (S-T-S) in all bacterial arginine-, cysteine-, and asparagine-specific mono-ARTs and eukaryotic ecto-ARTs. By opposition, on ARTDs and diphthamide-specific ARTs, this motif is found as Tyrosine-X-Threonine/Serine or Tyrosine-Phenilalanine/X-Alanine/X. The last motif is distributed between the ADP-ribosylating turn-turn and the adjuring β-strand. This motif contains the catalytic glutamate and the Glutamine/Glutamate-X-Glutamate (Q/E-X-E)**,** present in bacterial arginine-, cysteine-, asparagine-, and guanosine-specific ARTs, as well as arginine-specific ecto-ARTs and bacterial diphthamide-specific ARTs (Hottiger et al., 2010).

From these three motifs, there are three amino acids essential for the NAD^+ to bind and for the reaction to occur. The Histidine (H) from the first motif, Tyrosine (Y) from the second and Glutamate (E) form the H-Y-E triad for the diphtheria toxin, exotoxin A, cholix toxin and all eukaryotic ARTs catalysing PARylation while for the Arginine-, cysteine-, asparagine-specific ARTs, as well as the ecto-ARTs, the triad is composed of the Arginine

(R), Serine (S) and Glutamate (E), R-S-E, from the first, second and third motif, respectively (Cohen & Chang, 2018; Hottiger et al., 2010).

Although PARPs belong to the ARTDs and should contain an H-Y-E triad in their ADPR fold, only 6 of the existing 17 have the HYE motif. In the other 11, the glutamate is replaced by I, L, V or Tyrosine. As this glutamate and other residues required for formation of poly-ADP-ribose chains are absent in these PARPs, they are thought to be only able MARylate their targets (Table 1)(Aravind et al., 2014; Hottiger et al., 2010).

Table I – ARTDs activity, domains and cellular location. (Aravind et al., 2014; Hottiger et al., 2010)

Enzyme	Activity	Catalytic domain	Location	Non-ART Domains
ARTD1/PARP1	Poly-ADPR	H-Y-E	Nucleus	PRD, WGR, AMD, BRCT, ZF
ARTD2/PARP2	Poly-ADPR	H-Y-E	Nucleus and cytoplasm	PRD, WGR, SAP
ARTD3/PARP3	Mono-ADPR	H-Y-E	Nucleus and cytoplasm	PRD, WGR, NWE?
ARTD4/PARP4	Mono-ADPR	H-Y-E	Nucleus and cytoplasm	VWA, VIT, PRD-like, BRCT
ARTD5/PARP5a/Tankyrase1	Oligo-ADPR	H-Y-E	Nucleus and cytoplasm	SAM, ARD, HPS
ARTD6/PARP5b/Tankyrase2	Oligo-ADPR	H-Y-E	Nucleus and cytoplasm	SAM, ARD
ARTD7/PARP15	Mono-ADPR	H-Y-L	Cytoplasm	A1pp/macro
ARTD8/PARP14	Mono-ADPR	H-Y-L	Nucleus and cytoplasm	WWE, A1pp/macro, RRM
ARTD9/PARP9	No activity**	Q-Y-T	Nucleus and cytoplasm	A1pp/macro
ARTD10/PARP10	Mono-ADPR	H-Y-I	Nucleus and cytoplasm	UIM, GRD, RRM
ARTD11/PARP11	Mono-ADPR	H-Y-I	Nucleus and cytoplasm	WWE
ARTD12/PARP12	Mono-ADPR	H-Y-I	Nucleus and cytoplasm	WWE, ZF/THP, ZF
ARTD13/PARP13	No activity**	Y-Y-V	Cytoplasm	WWE, ZF/THP, ZF
ARTD14/PARP7	Mono-ADPR	H-Y-I	Nucleus and cytoplasm	WWE, ZF/THP
ARTD15/PARP16	Mono-ADPR	H-Y-Y	Cytoplasm	TMD
ARTD16/PARP8	Mono-ADPR	H-Y-I	Cytoplasm	HPS
ARTD17/PARP6	Mono-ADPR	H-Y-I	Cytoplasm	HPS

In eukaryotic cells, more players involved in the ADP-ribosylation picture have emerged. ADP-ribosylation is met in a balance between “writers”, “readers”, “erasers”, “feeders” and “consumers” (Gupte et al., 2017). “Writers” are, obviously, the ARTs, which transfer the ADP-ribose to the target protein, the ADP-ribose binding domains (ARDBs) the “readers”, the ADP-ribose and PAR glycohydrolases (PARGs) the “erasers” (PARG, ARH3, TARG, MacroD1, MacroD2, NAD^+ synthases the “feeders” and the enzymes which have NAD^+ as a substrate the “consumers” (PARPs, Sirtuins, NADases, CD38) (Gupte et al., 2017).

Many proteins have ADP-ribose binding domains in their structure to allow the signalling pathways to occur and, as such, are involved in DNA-damage repair, oxidative stress response and other mechanisms and functions (Palazzo et al., 2017). The main domain

studied is the macrodomain. Macrodomain-containing proteins can recognize PAR and MAR residues in many different targets of ADP-ribosylation (Palazzo et al., 2017). One kind of macrodomain, PAR glycohydrolase (PARG), can remove the ADP-ribose domain. PARG can cleave the O-glycosidic bond between riboses, and therefore, can reduce the PAR to MAR. However, it is not able to remove the first ADP-ribose added to the protein. This moiety can only be removed by other hydrolases like MacroD1, MacroD2 or terminal ADP-ribosyl glycohydrolase1 (Palazzo et al., 2017). Other ARBDs include PAR-binding motifs (PBMs), PAR-binding zinc finger (PBZ) modules, and WWE domains (Gupte et al., 2017). Some of these ARBDs have been used as tools for studying the role of ARTs in cells.

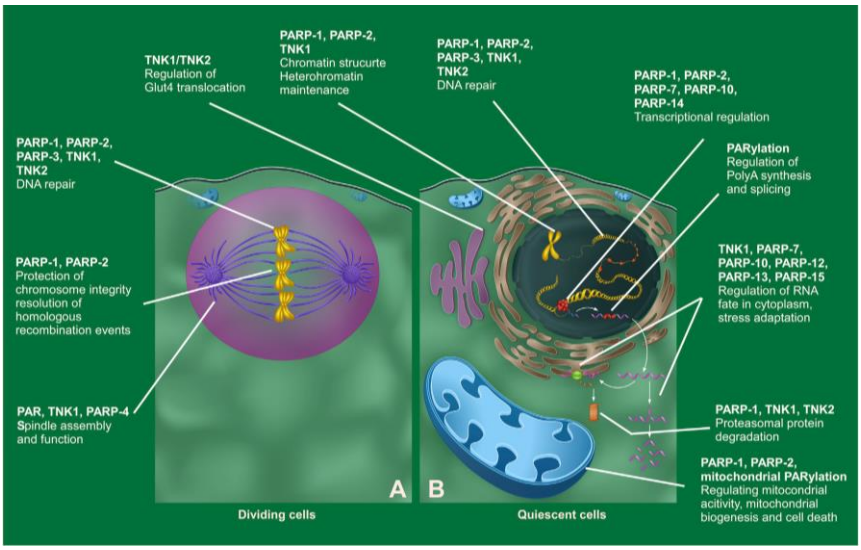

Figure 2 – Overview of PARPs functions in cells (Bai, 2015)

Endogenous ARTs have been correlated to multiple function on the cells, the help regulating the cell stress response to DNA damage, cytoplasmic stress responses They are involved in process as modulation of gene expression, mRNA stability, gene expression (Gupte et al., 2017).

PARP1/ARTD1, the first identified and the most studied of the endogenous ARTs, is a nuclear PARP involved in multiple functions related to DNA damage repair, cell death, gene expression and regulation and RNA suppression (Gupte et al., 2017). PARP1 role in DNA damage repair is present for both single-stranded breaks (SSB) or double-stranded breaks (DSB)(Wei & Yu, 2016). In SSB, PARP1 senses the damage and auto-ADP-ribosylates itself (Kim, Zhang, & Kraus, 2005). Now, PARP1 has poly-ADP-ribosylating activity and the polymers formed by it can go until 200 units (Wei & Yu, 2016). This creates quite a big

signal of negative charge density, allowing the ARDB present in other proteins to bind and also to act as a scaffold protein to the assembly of DNA damage repair complexes (Cohen & Chang, 2018; Wei & Yu, 2016). The SSBR factor X-ray repair cross-complementing protein 1 (XRCC1) is an example of that as it binds with the PAR branches and is recruited to the DNA damage site (Wei & Yu, 2016).

As for the DSB repair, PARPs major role is through the ADP-ribosylation of the histones, potentiating the expansion of compacted chromatin allowing the repair machinery work more competently (Gupte et al., 2017). If the stress is too much, PARP1 may initiate cell death known as *Parthanatos* which independent of caspases (David, 2009). The intensity of the signal by PARP1 determines the cellular outcome, either DNA repair and cell survival or senescence or cell death (Luo & Lee Kraus, 2012).

Other nuclear PARPs as PARP2/ARTD2 and PARP3/ARTD3 also play a role in DNA damage repair, as PARP3 is important for DSB repair working synergistically to potentiate NHEJ at DSB sites (Gupte et al., 2017). However, PARP2 and PARP3 activation requires the DNA to be 5'-phosphorilated (Langelier, Riccio, & Pascal, 2014).

New roles have emerged for PARPs and recently ADP-ribosylation has been linked to ubiquitination in 2 distinct ways. One where the PARylation of a target protein by PARP1 or PARP5/ARTD5 allowed the recruitment of RNF146, a ubiquitin E3 ligase containing a WWE domain (Gupte et al., 2017). The identification of a new mechanism of ubiquitination without E1 and E2 in *Legionella pneumophila* spreads the range of possible targets as well as provide with another PTM mechanism used by bacteria to influence the host to its advantage (Kotewicz et al., 2017).

As for the MARylating PARPs, some of their functions speak of the continuous fight between pathogen and host as many of them are responsible for responses to stress. Starting with PARP10/ARTD10 whose activation leads to attenuation of NF-κB during viral infection (Verheugd et al., 2013). PARP13/ARTD13 on the other hand promotes innate antiviral defences by TRAIL-mediated apoptosis and promoting accumulation of cytotoxic transcripts (Todorova, Bock, & Chang, 2014).

Together with Deltex E3 ubiquitin ligase 3L, PARP9/ARTD9 can mediate immune responses to viruses as well as stimulate the degradation of viral proteases (Yang et al., 2017). And, upon, stimulation by type II interferons, the expression levels of PARP12/ARTD12 were increased as well as Ectopic expression of PARP12 leads to

increased NF-κB signalling (Welsby et al., 2014). Additionally, another role for PARP1 might be related to inflammation and stress response as PARP1-null mice were found to be resistant to septic shock due to the decreased levels of proinflammatory cytokines (Gupte et al., 2017) On the other hand, loss of PARG during HSV-1 replication suggests that increases in PARylation could promote viral infection (Grady, Hwang, Vastag, Rabinowitz, & Shenk, 2012).

PARP14/ARTD8 has been liked to immune cells functions and differentiation. Additionally, it is also important for adhesion, cell motility and survival. In macrophages PARP14 inhibits proinflammatory response to IFNγ stimuli as well as enhancing anti-inflammatory response to IL-4 (Iwata et al., 2016). In multiple myeloma, PARP14 inhibits JNK1 and promotes the cancer cells survival (Barbarulo et al., 2013).

PARP9 was recently identified to bind to Dtx3L and together ADP-ribosylate ubiquitin (Yang et al., 2017). Lastly, PARP13 have been found to be catalytic inactive and no activity has been reported yet (Gupte et al., 2017). However, it was found that PARP9, PARP14 or PARP15/PARP7 knockdown actin cytoskeletal defect while PARP13 knockdown showed viability defect.

2. Salmonella

Salmonella comprises a large group of Gram-negative bacterial pathogens responsible for bacterial gastrointestinal infections in mammals. *Salmonella*-caused diseases can range from intestinal inflammation and diarrhoea to typhoid depending on the host susceptibility and the serotype of the bacteria (Fàbrega & Vila, 2013). *Salmonella enterica* serovar Typhimurium is a facultative intracellular subtype of *S. enterica*, which actively invades host cells and resides within a membrane-bound compartment called the *Salmonella*-containing vacuole (SCV) (Fàbrega & Vila, 2013). *Salmonella* infection begins when the bacterial cells attach to the intestinal epithelium. Bacteria is, then, engulfed by the host cell into the SCV, either in epithelial cells or M cells. Additionally, *Salmonella* can also cross the epithelium via the dendritic cells (Fàbrega & Vila, 2013). When inside the cell, the bacteria replicate and survive. In epithelial cells, *Salmonella* is transcytosed to the submucosa, whereas in M

cells, phagocytes internalize the pathogen where they reside within another SCV. The phagocytes then spread the bacteria along the nymph and blood stream (Fàbrega & Vila, 2013).

After internalization and replication with the cell, *Salmonella* is released to the extracellular for system spread (Fàbrega & Vila, 2013). In epithelial cells, cell death occurs by an apoptosis-like mechanism, where the plasmatic membrane is kept intact to prevent inflammatory response. The machinery involved in this process is T3SS-2 and caspase-3, independent of caspase-1 (Fàbrega & Vila, 2013). The *Salmonella* SPI-1 mediate macrophage death by pyroptosis, which is a cell pathway where caspase-1 is activated, independent of caspase 3 and 8, releasing interleukine-1β and interleukine-18, promoting inflammation and subsequent phagocytosis by newly arrived macrophages (Blériot & Lecuit, 2016). These macrophages will, then, help the systemic spread of *Salmonella* (Fàbrega & Vila, 2013).

Salmonella encodes two virulence-associated type III secretion systems (T3SSs), T3SS-1 is encoded within *Salmonella* pathogenicity island 1 (SPI-1), the first of five (Fàbrega & Vila, 2013). T3SSs are used by many Gram-negative pathogens to deliver bacterial effector proteins into host cells, responsible for invasion, induction of inflammation, intracellular survival and replication (Agbor & Mccormick, 2011). *Salmonella* SPI-1 is important for bacterial invasion using effectors like SopE, SopE2 and SopB to perturb the cell actin organization and entry the host cell. In turn, SptP has the opposite effect and stimulates the closing and rearrangement of the actin to the original status allowing the internalization of *Salmonella* (VanEngelenburg & Palmer, 2008). SPI-2, on the other hand, is of very important for *Salmonella* survival and replication within the SCV, ejecting the effectors by the second T3SS, expressed among its genes. The other SPI have not been studied to such detail; however, it is known that SPI-3 expresses proteins that act in accordance with SPI-1 and SPI-2, while SPI-4 expresses a protein associated with the interaction with the epithelial cells in the beginning of infection. SPI-5 is required for pathogenic processes and contributes to systemic infection (Fàbrega & Vila, 2013).

Among *Salmonella*s genetic material lies a plasmid containing a virulence genes (*spv*) region with five genes (Tezcan-Merdol et al., 2001). As this *spv* is highly conserved and present in many different serovariants, it is concluded it must be essential to the plasmid virulence and it is, as well as, in the whole of *Salmonella* (Tezcan-Merdol et al., 2001). Indeed, the removal

of these genes, reduces plasmid virulence. Among the five genes present in the *spv*, there is the *spvB*, a mediator of bacterial intracellular proliferation effector protein associated with *Salmonella* proliferation in macrophage (Tezcan-Merdol et al., 2001). SpvB protein has ADP-ribosyl transferase activity, and it acts as an intracellular toxin, which covalently modifies monomeric actin (Tezcan-Merdol et al., 2001). This modification leads to loss of F-actin filaments and cytoskeleton depolymerization in *Salmonella*-infected human macrophages. SpvB represents then the use of ADP-ribosylation of actin by bacteria to favour their intracellular growth (Tezcan-Merdol et al., 2001).

SpvB is the first ADP-ribosylating enzyme shown to be a virulence factor for an intracellular pathogen. As *Salmonella* grow within an intracellular vacuole, SpvB acts through local or global actin depolymerization, which affects either vesicular trafficking or cellular physiology, or both, to promote *Salmonella* proliferation. Ultimately, this cytotoxicity leads to apoptosis, which could promote cell-to-cell spread of *Salmonella* by phagocytosis of infected, apoptotic cells (Lesnick, Reiner, Fierer, & Guiney, 2001). Additionally, it was described a pertussis-like toxin within the effectors proteins of *Salmonella* Typhimurium capable of ADP-ribosylate G proteins in Chinese hamster ovary cells (Uchida et al., 2009). ADP-ribosylated G proteins are then continuously active, increasing the levels of cyclic AMP and disrupting of their regulatory activity (Uchida et al., 2009). Despite the growing numbers of studies done with ADP-ribosylating toxins, the role on the endogenous ADP-ribosylating activity during infection has not been studied.

Chapter II – Objectives

Post-translational mechanisms are a relevant part of the cell functions as many of them act in response to environmental changes. Bacterial infection is one major cause of stress to the host cell. This project is based on a hypothesis that endogenous host cell PARPs become activated in bacterial infection and ADP-ribosylate specific host cell proteins to regulate cell functions. Activation of PARPs in host cell during infection might either benefit the invading bacterium or the human host.

With this work, I aim to:

1. Detect ADP-ribosylated proteins in infected, LPS- or cytokine-treated cells.

ADP-ribosylated proteins will be detected with Western blotting-based approaches using cells of infected or LPS- and cytokines-treated epithelial and macrophage cell lines.

2. Quantify expression levels of PARPs in infected, LPS- or cytokine-treated cells.

Expression levels of selected PARPs will be quantified with qPCR and Western blotting using cells of infected or LPS- and cytokine-treated epithelial and macrophage cell lines.

Chapter III – Materials and methods

1. Cell culture and bacterial strains

HeLa 229 (ATCC® CCL-2.1™) were cultured in DMEM media supplemented with 10% FBS, 2 mM L-glutamine and penicillin-streptomycin (Gibco) at 40 U/ml and THP-1 (ATCC® TIB202™) were grown in RPMI 1640 (Lonza™ BioWhittaker™) supplemented with 10% FBS, 2 mM L-glutamine at and penicillin-streptomycin (Gibco) at 40 U/ml at 37°C under 5% CO_2 humified atmosphere. *Salmonella enterica* serovar Typhimurium SL1344 strain (Barthel et al., 2003) and *Shigella flexneri* (ATCC® BAA2402™) was used for bacterial infection.

a. Transformation of *Salmonella* with pAhC-EGFP plasmid

Salmonella was grown overnight in 5 ml Luria Broth (LB) and *Shigella* in 5 ml of Trypticase Soy Broth (TSB). Both were reinoculated the next day as 1:10 in 5 ml of LB/TSB and grown at 37°C shaking until OD_{600}= 0.7. After cooling in an ice-water bath for 15 min, bacterial cells were centrifuged at 4000 x g for 10 minutes at 4°C. They were firstly washed with 5 ml of HEPES (10 mM, pH 7.0) and secondly with 50 µl of 10% glycerol. Lastly, they were resuspended in 40 µl of 10% glycerol.

20 ng of plasmid pAhpC-EGFP (Pulliainen, Hytönen, Haataja, & Finne, 2008) was added to the electrocompetent cells and electroporation was run in 2 mm gap cuvette at 2500 V. After incubation at 37 °C for an hour, bacterium was plated in LB plates with 50 µg/ml kanamycin.

b. Differentiation of THP-1 cells

THP-1 cells were seeded two days prior to experiment at a concentration of $1x10^6$ cells/ml in RPMI medium supplemented with 10% FBS, ultra-glutamine, pen-strep and 10 ng/ml of phorbol 12-myristate 13-acetate (PMA) (P8139). After 24 hours, cells were washed twice with phosphate buffered saline (PBS) (2 mM NaH_2PO_4, 8 mM NaCl) and added fresh RPMI media without PMA. After resting for 24 hours, cells were washed again with PBS and added new media.

2. Infection set up for cell lines with *Salmonella* and *Shigella*

Cells were seeded the previous day in 6-well plates at a concentration of $6.6x10^4$ cells/ml in their respective media. Next day, cells were washed with PBS and added fresh media without penicillin-streptomycin. *Salmonella* and *Shigella* were reinoculated from overnight growth

at a ratio of 1:50 to 7 ml of fresh medium, Luria Broth and Tryptic Soy broth, respectively, at 37°C and grown until OD_{600} was between 0.5-0.8, shaking. Afterwards, they were centrifuged for 5 min at 300 x g and resuspended in 1ml PBS. After repetition of centrifugation and resuspension, new OD_{600} value was measured in a 1:10 dilution. Bacteria was then added to the cells at a Multiplicity of Infection (MOI) value of 20 for *Salmonella* and 40 for *Shigella*. Cells and bacteria were incubated at 35°C and 5% CO_2.

3. Lipopolysaccharide (LPS) or cytokine stimulation

Cells were seeded the previous day in 6-well plates at a concentration of $6.6x10^4$ cells/ml in their respective media. Next day, cells were washed with PBS and added fresh media supplemented with 100 ng/ml of E. coli 0111: B4 strain derived LPS (tlrl-3pelps), 100 U/ml of IFNγ (PHC4031), 100 U/ml of IFNα (SRP4596) or 10 ng/ml of TNFα (210-TA). Samples were collected at 2, 8, 12, 24 and 48 hours after washing twice with PBS by trypsination. Later cells were lysed by NP-40 lysis buffer (50 mM Tris-HCl, pH 7,5; 1% NP-40 and 1x Protease inhibitor containing EDTA (Pierce™)). Afterwards, concentration was measured by Bradford assay (BIO-RAD).

4. H_2O_2 treatment

Cell were seeded the previous day at a concentration of 2.0x105 cells/ml in 20 mm plates. Next day, they were washed 2x with PBS and incubated for 10 min at 37°C and 5% CO2 in PBS supplemented with 400 µM of H_2O_2 (Merck Millipore). After incubation, plates were washed 2x with PBS and then samples were collected in either modified RIPA buffer containing PARP and PARG inhibitors (50 mM Tris-HCl, pH 7.5; 400 mM NaCl; 1 mM EDTA; 1x Protease inhibitor (Pierce™); 0,1% Na-deoxycholate; 75 µM tannic acid; 40 µM PJ34; 1% NP-40) or Laemmli dye (4 % SDS, 20% glycerol, 120 mM Tri-HCl, pH 6.8, 0.002% bromophenol blue).

5. Flow cytometry assay to quantify *Salmonella* infection efficiency

Using the infection method described in point 2, at time-points 1-6, 12 and 24 hours, wells were washed 3x with PBS and trypsinized. Flow cytometry data was acquired by BD Accuri C6 Flow cytometry instrument (BD Biosciences, San Diego, CA) and data analysed using BD Accuri C6 software.

6. Western blotting-based assay to visualize ADP-ribosylated proteins in *Salmonella*- and *Shigella*-infected cells

During infection, cells were either collected in modified RIPA buffer containing PARP and PARG inhibitors (50 mM Tris-HCl, pH 7.5; 400 mM NaCl; 1 mM EDTA; 1x Protease inhibitor (#88666); 0,1% Na-deoxycholate; 75 µM tannic acid; 40 µM PJ34; 1% NP-40) or 2x Laemmli dye. Proteins were resolved in 10-15 % SDS-PAGE gels and transferred to nitrocellulose membranes. Blocking was done with BSA or milk according to antibody manufacturer specificities. For detection of ADP-ribose-attached proteins, antibodies used were rabbit anti-PAR polyclonal (Enzo ALX-210-890A), Additionally, a macrodomain from the protein Af1521 from archaebacteria *Archaeoglobus fulgidus* tagged with a GST tag was used to detect MAR as well as the terminal ADP-ribose of PAR. As such, an anti-GST was needed to detect the macrodomain, it was used monoclonal anti-GST (MA4-004) antibody. Loading controls were done with anti-actin (SC-1616), anti-GAPDH (ab9485) or Ponceau stain. Detection was done using Westernbright HRP substrate (Advansta) and ImageQuant LAS 4000 (GE Healthcare).

7. Quantification of expression levels of PARP1 and PARP14 during *Salmonella* infection and lipopolysaccharide (LPS) or cytokine stimulation

Based on samples collected from infection with *Salmonella* and LPS or cytokine stimulation, Western-blot was performed to detect PARP1 and PARP14 using monoclonal anti-PARP1 (SC-8007) and anti-PARP14 (SC-377150), anti-ICAM1 (sc-8439) for positive control and anti-actin (SC-1616) and anti-GAPDH (ab9485) for loading control. PARP1 can be detect in two forms: at 116 kDa, full length, 89/24 kDa, C-/N-terminal cleavage products. PARP14 has 5 isoforms described with sizes of 202 kDa, 193 kDa, 170 kDa, 189 kDa and 89 kDa being the first one the canonical one.

For quantification of *parp1* and *parp14*, samples were collected, after infections, with trypsin and RNA was isolated with NucleoSpin® RNA (MACHEREY-NAGEL). Concentration of RNA was measured by Nanodrop (Thermo Fisher). 1 µg of RNA was converted to cDNA using SuperScript™ III Reverse Transcriptase (Invitrogen™). qPCR was assembled with Kapa Probe Fast and the primers described in the table below. Universal probes from Universal ProbeLibrary. qPCR run and analyses were performed using QuantStudio 12K Flex software. Relative mRNA expression levels of targeted genes were normalized to expression levels of the housekeeping gene (GAPDH) and estimated using comparative ΔΔCt method.

Table II – Primers sequence used for qPCR

Gene	Sense primer	Antisense primer
Parp1	TCTTTGATGTGGAAAGTATGAAGAA	GGCATCTTCTAAGGTCGAT
Parp14	GTGTTCTTCTACCCGGAGGA	TTCCTTGCCATACCAACTCA

a. Isolation of white cells from human blood

Blood was collected from healthy donor fresh in the day of infection into EDTA-coated collection tubes. Whole blood was centrifuged at 500 g for 10 minutes, at room temperature. Buffy coat was then collected from fractionated blood and incubated with red blood cells lysis buffer (1,5 M NH_4Cl, 0.1 M $NaHCO_3$ and 10 mM EDTA) pre-heated to 37°C for 10 minutes. After repeating the centrifugation and RBCs lysis, cells were washed twice with PBS and finally resuspended in RPMI media supplemented with ultra-glutamine and 10% FBS. Cell count was done with Trypan Blue dye 0,40% (Bio-Rad) in counting slides on TC20™ automated cell counter (Bio-Rad).

8. Treatment of bacterial lysates with hydroxylamine

Bacterial lysates from *Salmonella* and *Shigella* were treated with fresh hydroxylamine at a final concentration of 1 M and incubated overnight at room temperature. Next day, the reaction was stopped with the addition of 3x Laemmli dye followed by boil at 95°C.

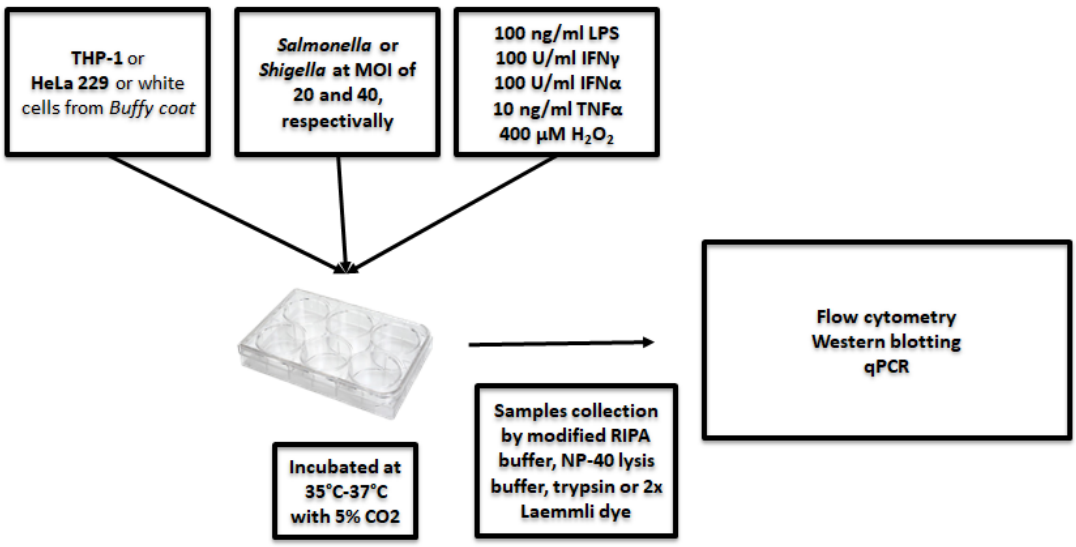

Figure 3 – Graphic representation of the work set-up.

This work belongs to a continuous project aimed to unravel the functions of endogenous ADP-ribosylation. This work was done with the contribution of Master Moona Miettinen and hence the presence of results involving *Shigella* infection.

Chapter III – Results

1. *Salmonella* and *Shigella* infect HeLa 229 cells

In order to first determine whether *Salmonella* and *Shigella* can infect HeLa 229 cells (ATCC® CCL-2.1™), a flow cytometry-based assay using GFP-expressing *Salmonella* and *Shigella* was done. The replicating pAhpC-EGFP plasmid is constitutively expressing GFP (Pulliainen et al., 2008). As bacteria infects cells, either by adhering to the cell surface or by invading the host cell, the signal from GFP within the cells is detected by the flow cytometer. This initial assay was necessary to assess if the set up was functional, at what time was the infection fully set and what would be the optimal conditions for it.

In these results (Figure 3) we initially saw the switch of the signal in bacterial samples expressing or not GFP protein (Figures 3 - A1-2 and B1-2). For *Shigella* while in A1 there is none in the quadrant above and 100% in the one below, in A2 there is a 68.3% increase in signal. As for *Salmonella*, the B1 also showed no signal while B2 showed 23.8% corresponded to GFP-positive bacteria. As such, we can used transformed bacteria to infect.

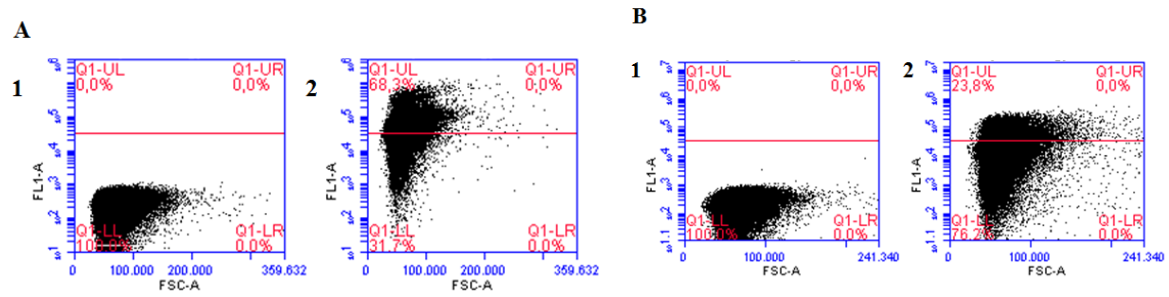

Figure 4 – Bacteria is expressing the GFP and is detect by the cytometer. (A) WT (A1) and GFP-expressing (A2) *Shigella*; (B) WT (B1) and GFP-expressing (B2) *Salmonella*;

Following are the samples of cells non-infected (Figures 4A and 5A) and those exposed to *Salmonella* (Figures 4C and 5C) and *Shigella* (Figures 4B and 5B) from 1 to 6 hours in DMEM media supplemented with 10% FBS and not supplemented. In all control samples at every time point we saw the value of events does not higher than 0.2%. On the other hand, bacterial-infected samples show a progressive increase. *Shigella* samples supplemented with FBS start with 0.4% in the upper right quadrant in the first hour (Figure 4) and stay around that percentage until the forth hour (Figure 4-B4) when it increases to 1.9% and to 4.2% in the following hour (Figure 4-A5). However, at the last time point (Figure 4-A6) the value drops to 3.7%. In non-supplemented *Shigella* infected samples, they follow the same initial

trend of having an unchanged first 3 hours followed by the increase at the 4 hours' time point (Figures 5 - B1-4), however here we saw a clearer increase until the 6th hour time point (Figures 5 - B1-4) where it reaches the 12.5% of GFP-associated cells.

As for *Salmonella*-infected cells, the same can be seen. Both with and without FBS show a slow start at 0.3%. In cells supplemented with FBS, there is a steady increase for the first 4 hours of infection (Figures 4-C1-4), however, at the fifth hour there is a sudden increase to 24.7% (Figure 4-C5) and at the last time point to 58.7% (Figure 4-C6). In non-supplemented cells, the increase is steadier, with the 9.4% at the forth hour point (Figure 5-C4) and then 23.5% (Figure 5 - C5) at the fifth and lastly 32.9% (Figure 5 -C6).

Concluding, both bacteria can infect HeLa 229 cells, and such is visible by flow cytometry.

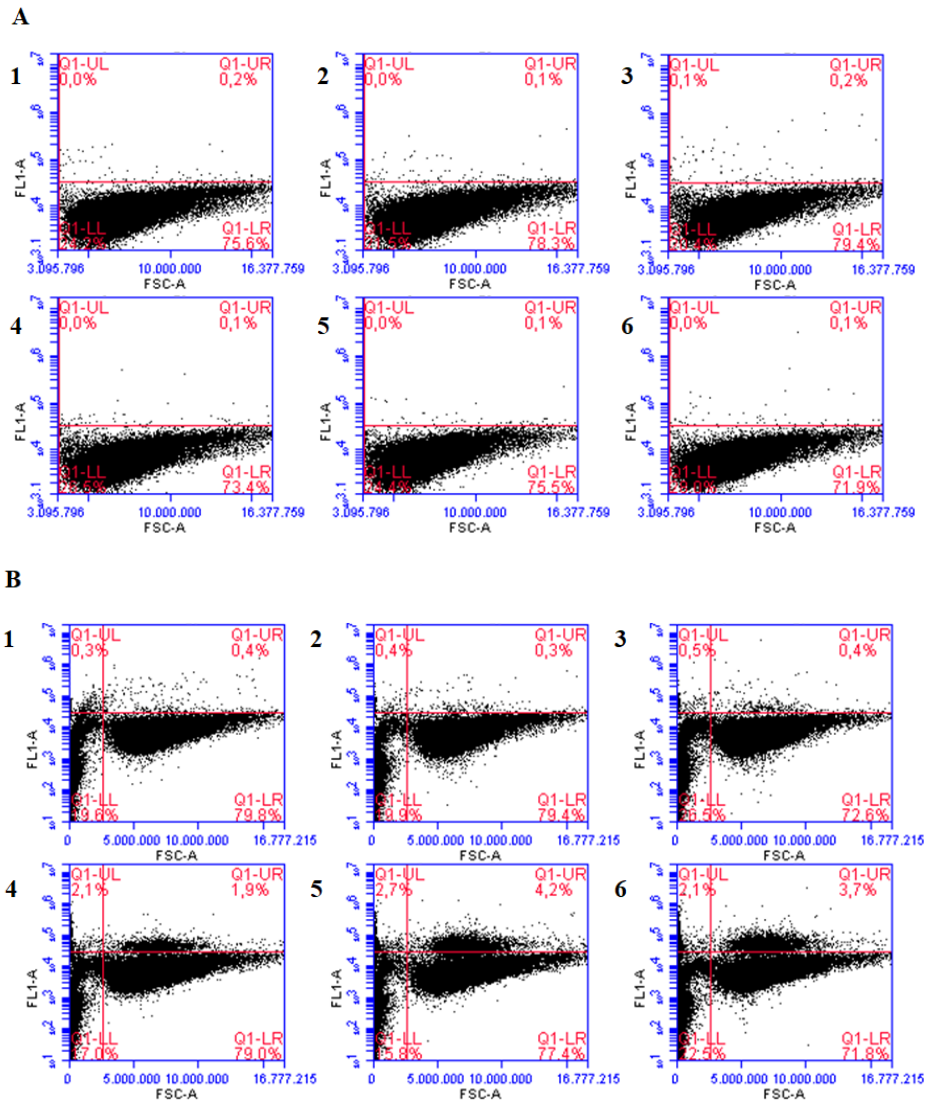

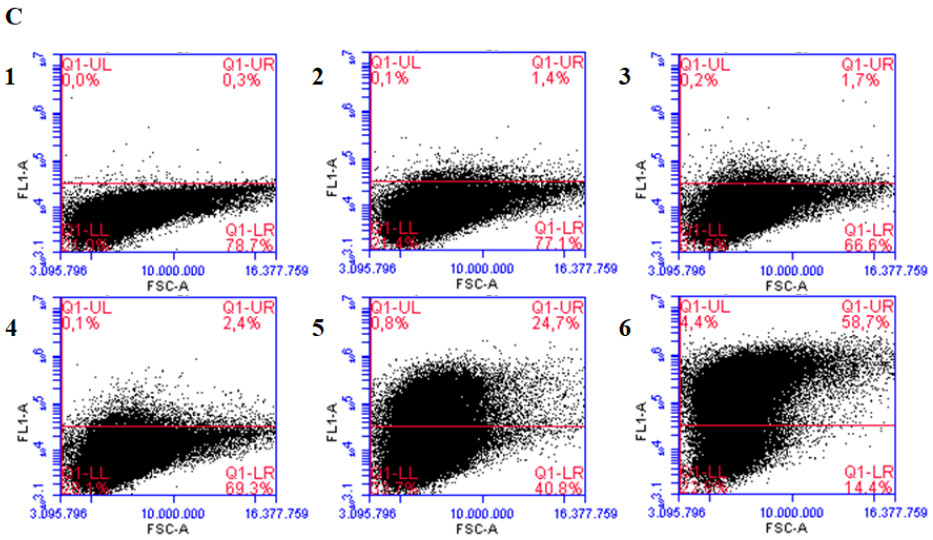

Figure 5 – Bacteria infect HeLa 229 cells in the presence of FBS. (A) HeLa 229 control cells supplemented with 10% FBS with A1 – after 1 hours, A2- after 2 hours, A3 – after 3 hours, A4 - after 4 hours, A5 – after 5 hours and A6 – after 6 hours; (B) *Shigella*-infected HeLa 229 cells supplemented with 10% FBS with E1-E6 corresponding to 1-6 hours, respectively; and (C) *Salmonella*-infected HeLa 229 cells supplemented with 10% FBS: G1-G6 are after 1-6 hours, respectively;

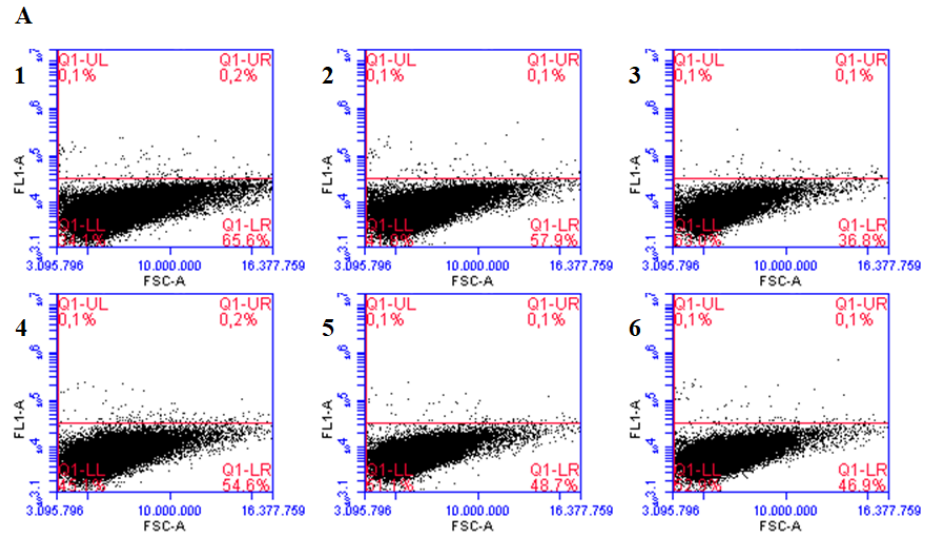

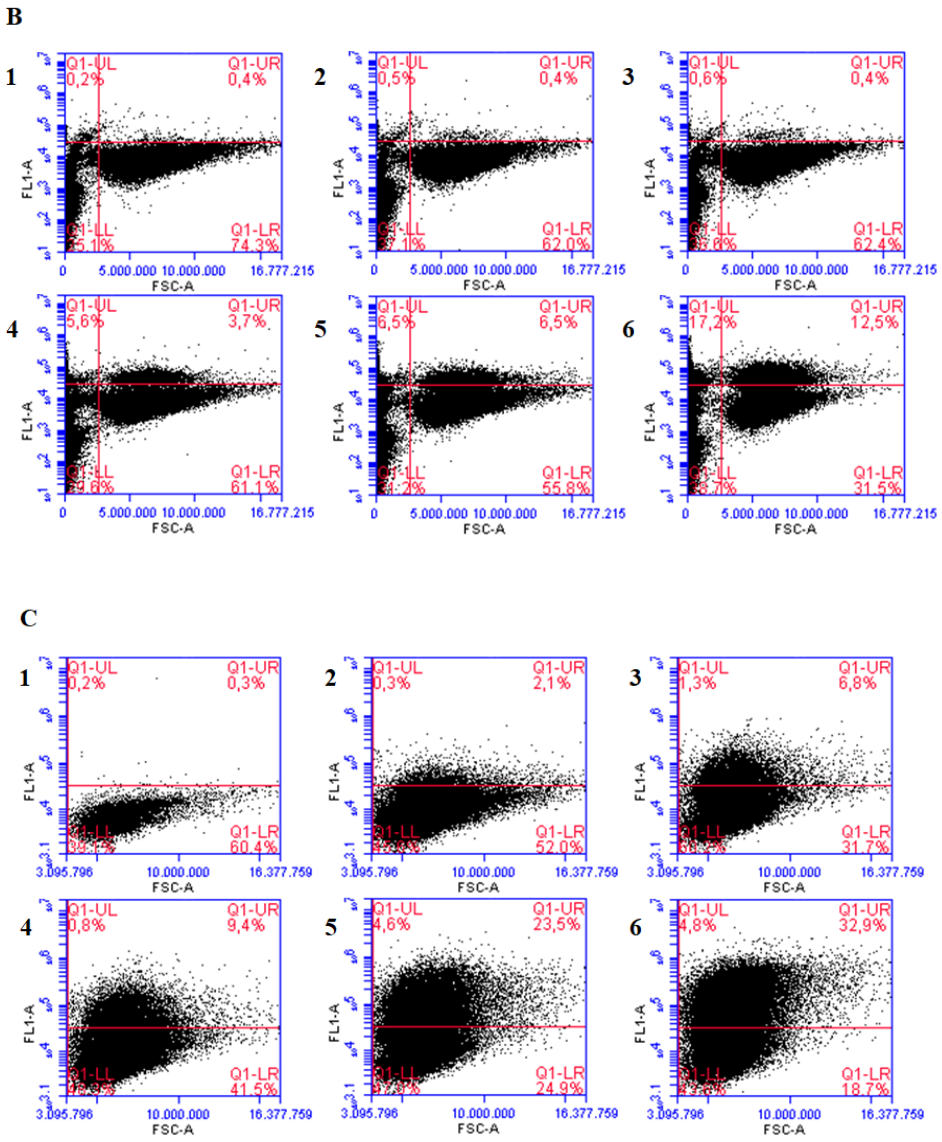

Figure 6 – *Shigella* and *Salmonella* infect HeLa 229 cells without the supplementation of FBS. (A) Control HeLa 229 cells not supplemented with FBS with D1-6 corresponding to 1-6 hours, respectively; (B) *Shigella*-infected HeLa 229 cells non-supplemented with FBS, F1-F6 is 1 to 6 hours respectively; and (C) *Salmonella*-infected HeLa 229 cells non-supplemented with FBS: H1-H6 corresponding to 1-6 hours infection.

2. HeLa 229 proteins are ADP-ribosylated by *Salmonella* and *Shigella*

For this experiment it was our interest to see any ADP-ribosylation signal that would be infection specific in HeLa 229 cells. In these initial blots we have samples corresponding to no infection and infection with *Shigella* or *Salmonella* from 1, 2, 3, 4, 5, 6, 12 and 24 hours. These samples were collected in the modified RIPA buffer.

As such, when probing with macrodomain Af1521 and anti-GST for the detection of mono-ADP-ribosylation, one band infection-specific is visible is between 35 and 55 kDa in the

Salmonella-infected samples at 12 and 24 hours (Figure 7). This band appears to increase in intensity as the infection progresses. In control samples probed with Af1521, we can also see a stronger band at 1, 3, 12 and 24 hours around 70 kDa (Figure 6 and 7).

When probing with the polyclonal anti-PAR we now see a lot a signal. In all lanes an unspecific band around 70 kDa. A lighter band shows at 120 kDa, at 3 and 6 hours, is present in both infection samples (Figure 8). In *Shigella*-infected samples we now have a band slightly above 70 kDa increasing intensity from 1 to 6 hours (Figure 8) but disappearing at the 12- and 24-hours' time point (Figure 9). Additionally, another band is visible slightly below 70 kDa in the first 6 hours of infection but lacking at 12 and 24 hours, this band is also similarly seen in *Salmonella*-infected samples. Furthermore, a band shows at 3 hours around 35 kDa remaining for the sixth hour but absent at 12 and 24 hours. Lastly, a band shows at 25 kDa constant at all time points (Figures 8 and 9).

As for *Salmonella*-infected samples, similarly to *Shigella* samples, we saw that same similar bands present in *Shigella* samples a little below 70 kDa and around 25 kDa, which starts to be visible at 3 hours and is present for the following time point samples at an increasingly intensity (Figures 8 and 9).

At the end of these results, it is visible that infection by either bacterium leads to multiple signals detected in HeLa 229 cells.

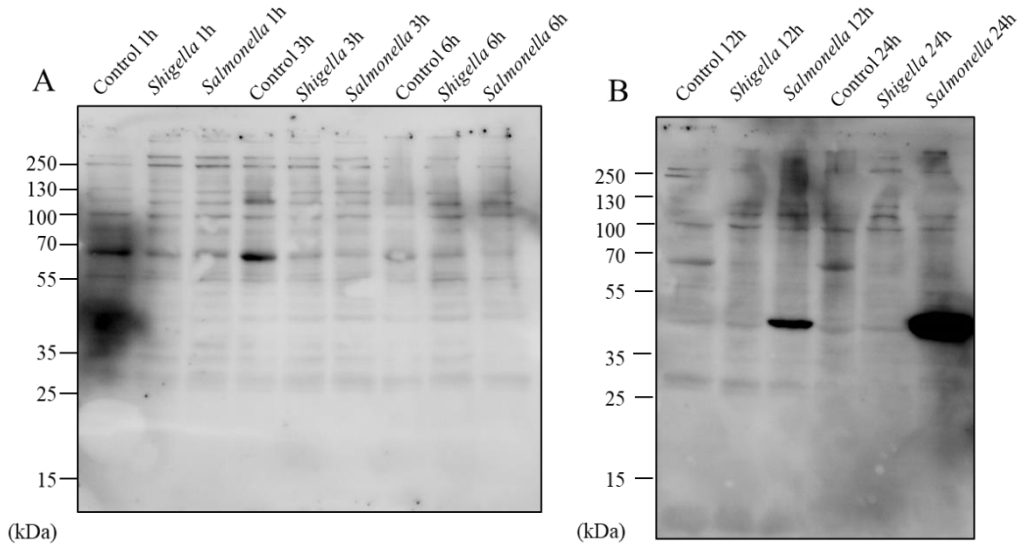

Figure 7 - Infection of HeLa 229 cells with *Salmonella* induced mono-ADP-ribosylation of protein sized between 35 and 55 kDa at 12 and 24hours. Probed with macrodomain Af1521 and polyclonal anti-GST antibody.

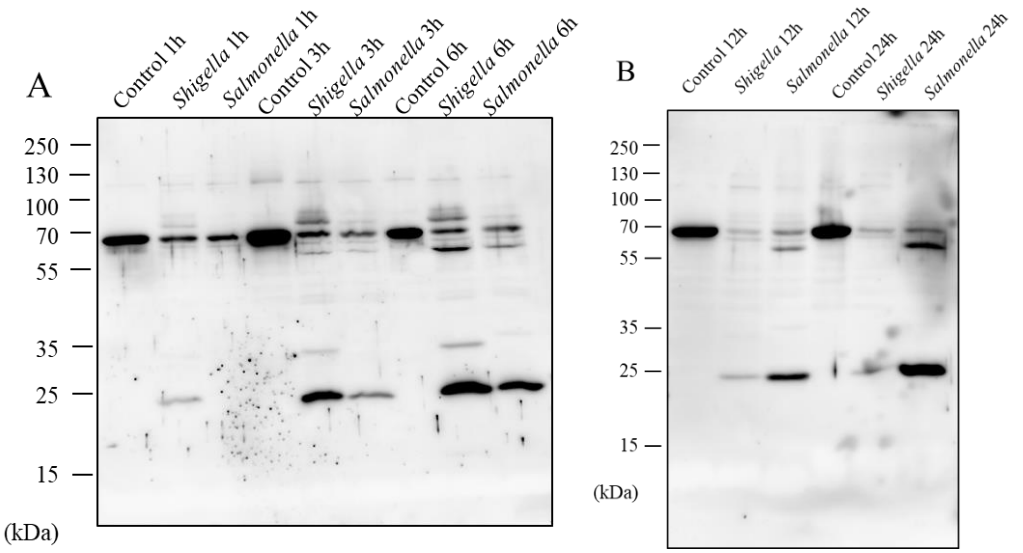

Figure 8 – Multiple signals detected for poly-ADP-ribosylation in HeLa 229 cells infected with *Salmonella* and *Shigella* in the first 6 hours of infection and in 12 and 24 hours after infection. Probed with polyclonal anti-PAR antibody.

a. 2x Laemmli dye optimal for sample collection.

PTMs are sensible to stress conditions and are quick to act. As it is in our interest to get the best possible result and keep the samples as unchanged as possible, we tested if colleting the samples in Laemmeli dye as opposing the RIPA buffer. In the latter we couldn't be sure that the tannic is indeed inhibiting the PARG activity as it is not its specific inhibitor (Bartolomei, Leutert, Manzo, Baubec, & Hottiger, 2016).

H_2O_2 is a strong stimulant of PARP activity (Robaszkiewicz et al., 2012). Cells under H_2O_2-induced stress activate PARP1 leading to necrotic cell death. As such we used samples collected under H_2O_2 effect as control samples. For that purpose, we collected control and H_2O_2-treated samples of HeLa229 cells with modified RIPA buffer and 1x, 2x and 3x Laemmeli dye (Figure 10).

In non-treated samples the cells under Af1521 probing show almost no signal from ADP-ribosylation whereas under the effect of H_2O_2 the whole lane profile changes with the appearance of multi signals.

In all untreated samples look quite similar sans a missing band at the highest point only present in RIPA buffer. Additionally, all Laemmeli dye-collected samples seemed to have a general faded look whereas control samples collected in RIPA buffer shows a stronger

signal. As for the H_2O_2-treated samples, those collected in Laemmeli had a much higher signal in the whole lane with increasingly intensity matching a higher concentration of Laemmeli dye.

This result led to change the protocol where from this point onwards samples would be collected by 2x Laemmeli.

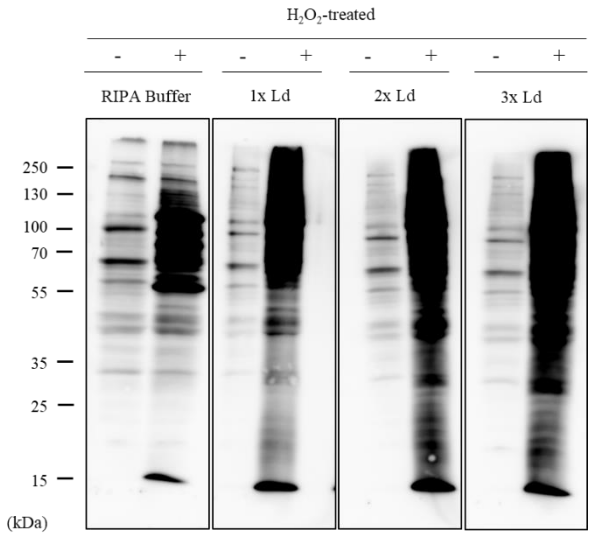

Figure 9 - Comparison between H_2O_2-treated HeLa cells collected with modified RIPA buffer and directly to Laemmli dye. Probed with macrodomain Af1521 and monoclonal anti-GST antibody.

b. Signals detected from infection unresponsive to PARP inhibitor

Next, we wanted to see if the bands we saw were due to endogenous ADP-ribosylation and not catalysed by bacterial proteins. With that purpose in mind, we incubated the cells, with and without bacteria, with 1 µM of Rucaparib, an inhibitor of PARPs. Samples were collected with 2x Laemmeli dye. First, we assessed if Rucaparib was active, for such, we added rucaparib to cells before H_2O_2-treatement. When supplemented with Rucaparib, H_2O_2-treated show a complete reversal of effect, with an almost no signal clear by Af1521 probing (Figure 11B). This result closely relates to control samples from non-H_2O_2-treated samples (Figure 11A).

When subjected to Rucaparib and probed with Af1521, after 6 hours of incubation, no difference was found between infected and non-infected samples (Figure 12A). Additionally, no effect is seen from Rucaparib as lanes from samples non-supplemented with the inhibitor seem the same as lanes from samples incubated with it, whether they were from bacterial-incubated cells or non-infected. At this point, the media was changed, and new media was added containing gentamycin as well as fresh Rucaparib. At 12 hours, a band is clear between 35 and 55 kDa in infection-associated samples (Figure 12B). Here Rucaparib seem to be active as signal present in the upper part of the lanes non-supplemented with the inhibitor is lost when it is present in the media. However, the band visible seems unaffected by Rucaparib. At 24 hours the blots seemed the same as at 12 hours (Figure 12C). The band seen before was still present and Rucaparib seemed still active as the same upper signal is lacking in Rucaparib-supplemented samples.

When probing with the polyclonal anti-PAR, we saw 4 signal which were infection-specific. One slightly higher than 70 kDa, one slightly below, one at 35 kDa and the last one at 25 kDa. The last three are clear to see from 6 hours infection time point onwards, while the first is only clear after 24 hours (Figures 12D-F). For the first 6 hours, it is not clear if the Rucaparib was working by this samples as no other signal besides the ones mentioned are visible and these didn't seem to show any fading Rucaparib-induced (Figure 12D). As for 12-hour time point samples, we saw a general fading of all signals as not even the signal previously clear at 70 kDa was very strong. Still, the signals slightly below 70 kDa, at 35 kDa and 25 kDa as still present (Figure 12E). Here we can see some signal present in infected samples not supplemented with Rucaparib at the higher weight size. This signal is lost when the cells were supplemented with the inhibitor. Lastly, the samples collected after 24 hours of infection show again the signal at 70 kDa more clearly (Figure 12F). Curiously, a higher than 100 kDa signal is shown that doesn't fade with Rucaparib while the same signal present in infected samples faded with the presence of Rucaparib. However, all the bands seen before are still present from 55 to 80, 35 and 25 kDa seemingly unaffected by Rucaparib (Figure 12F).

In conclusion, Rucaparib had not effect in the signals detect from untreated infection samples.

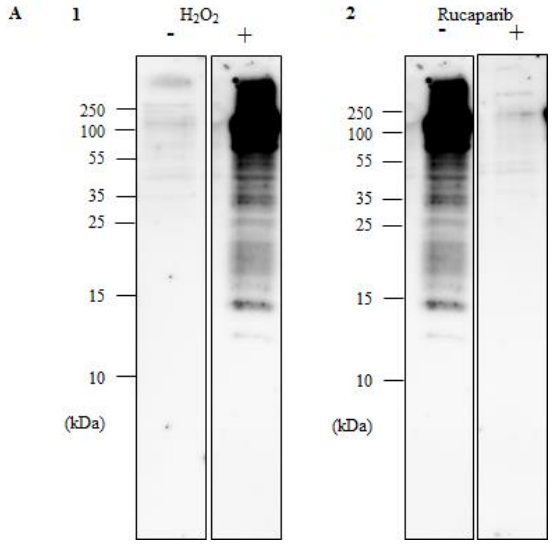

Figure 10 – PARP inhibitor eliminates H_2O_2-induced signal in HeLa 229 cells. H_2O_2-treated HeLa 229 cells without (1) and with Rucaparib supplementation (2). Samples collected in 2x Laemmli dye. Probed with macrodomain Af1521 and monoclonal anti-GST antibody.

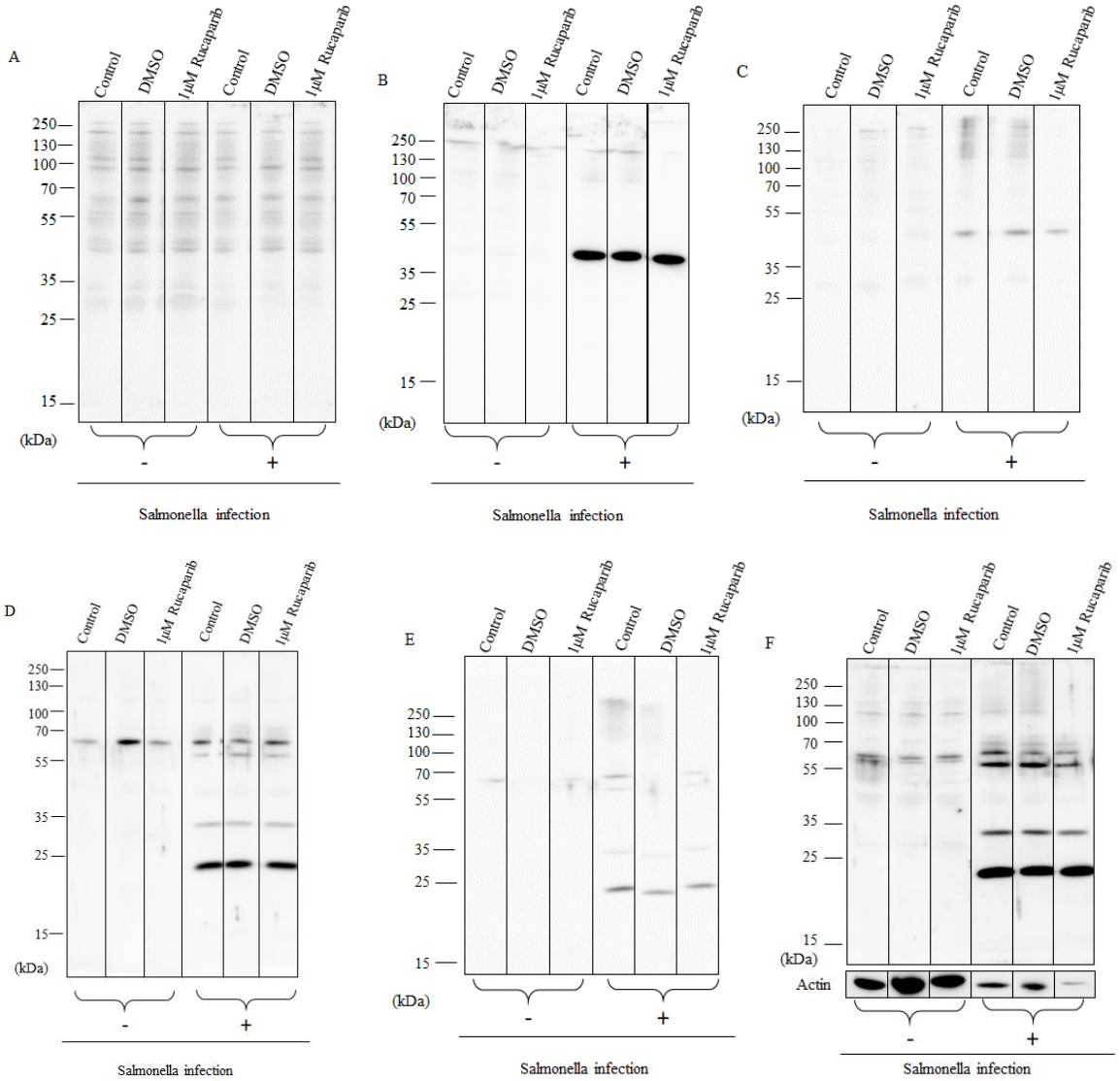

Figure 11- Rucaparib induced PARP inhibition ineffective against signals previously seen in HeLa 229 cells. *Salmonella* infection of HeLa 229 cells supplemented with Rucaparib, samples from 6 hours (A and D), 12 hours (B and E) and 24 hours (C and F). Probed with Af1521 and monoclonal anti-GST (A, B and C) and polyclonal anti-PAR antibodies (D, E and F).

c. Infection specific signals previously seen results from plain bacteria

As we saw due to the previous experiment that the signal was not due to endogenous PARPs, meaning the cells, we suspected that the signal would come from bacteria, or that it would be catalysed by the secreted bacterial ARTs. For that purpose, we added a new control to our blots this one containing just bacterial lysate grown in DMEM media.

We now see in the first two lanes after the molecular ladder the signal corresponding to plain bacteria. In these lanes, we see the same bands we previously saw in the paragraph above. When probing with the polyclonal anti-PAR and Af1521 no infection-specific signal is visible (Figure 13A-B). However, the signal that was clear before when probing the macrodomain is now visible when probing with the polyclonal anti-MAR. This signal found between 35 and 55 kDa, is clear is the samples originated from 12 hours infection (Figure 13C).

Finishing, we see multiple signals detected by anti-PAR antibody from plain bacteria and one signal from HeLa 229 cells infected with *Salmonella* from mono-ADP-ribosylation (Figure 13B).

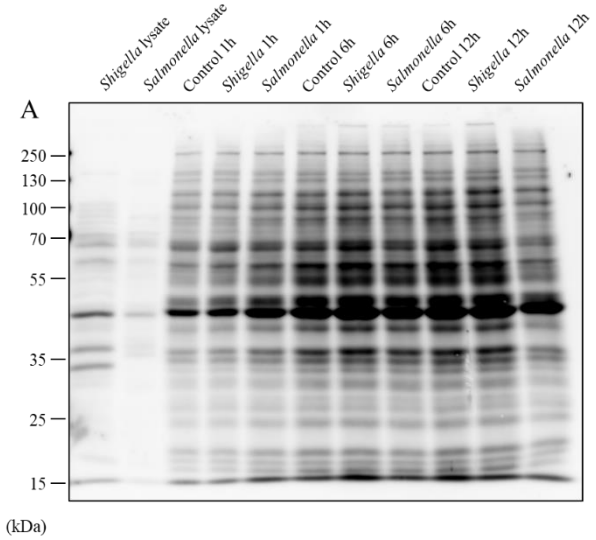

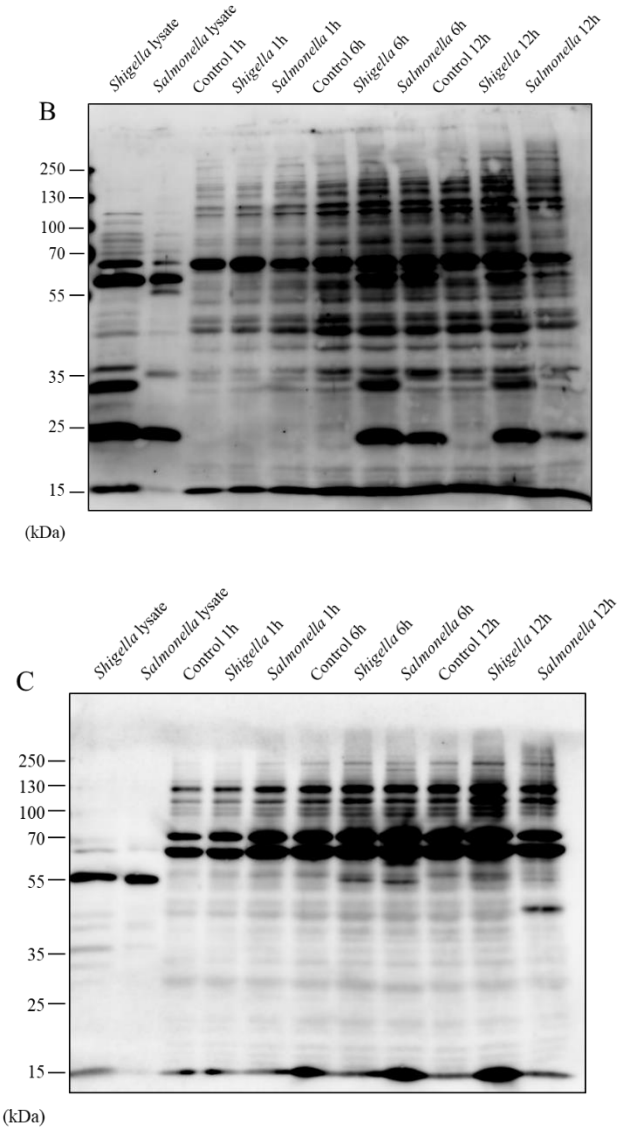

Figure 12 – Plain bacteria originated the signals previously seen except one mono-ADP-ribosylated protein from HeLa 229 cells. Probed with macrodomain Af1521 and monoclonal anti-GST (A), polyclonal anti-PAR (B) and polyclonal anti-MAR antibodies (C).

d. Hydroxylamine treatment produced no effect in bacterial signals

Hydroxylamine can remove ADP-ribose moieties from aspartate and glutamate amino acids (Zhang, Wang, Ding, & Yu, 2013). As such, we tested to see if using this treatment could help eliminate the signal we saw when probing the bacterial lysates with the polyclonal anti-PAR. Thus, we initially tested if the hydroxylamine was active, testing against H2O2-treated lysate and when treated with hydroxylamine, it is seen a decrease of signal in the lane when compared to non-treated with hydroxylamine.

Next, we now treated bacterial lysates from *Shigella* and *Salmonella* with hydroxylamine (Figure 14). The first obvious remark we made is the fact that both bacterial lysates look the same when previously many different signals were seen distinguishing one from other. Relative to the hydroxylamine effect itself, we saw no effect of it in the bands present in the blots as both the lanes of samples treated with hydroxylamine and those untreated appear unchanged in intensity.

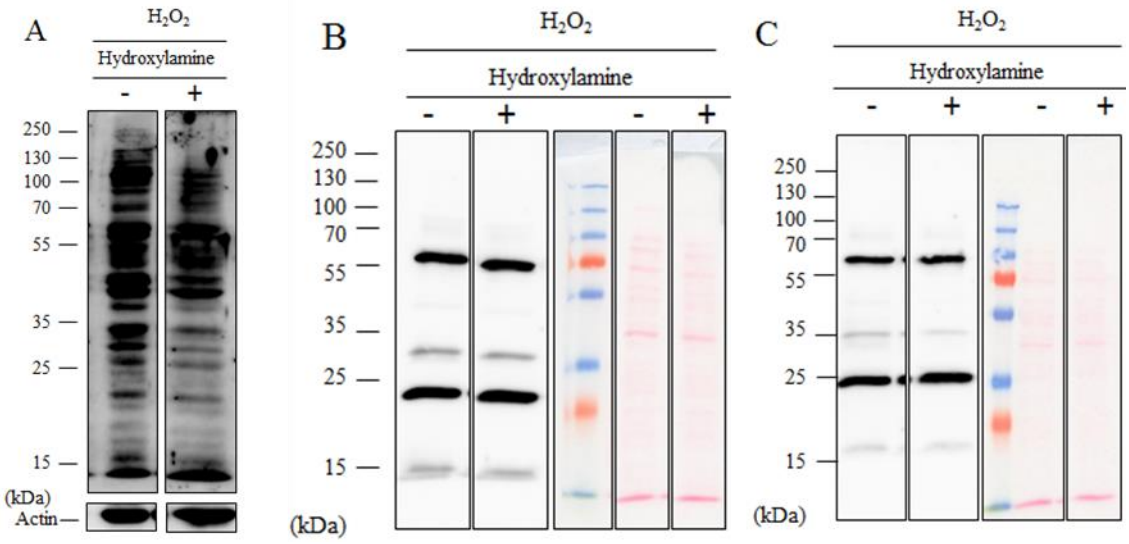

Figure 13 – Hydroxylamine ineffective against signals detected. H_2O_2-treated HeLa cells lysate (A), Shigella lysate (B) and Salmonella lysate (C) were treated with 1M of Hydroxylamine. Probed with polyclonal anti-PAR antibody or stained with Ponceau S staining.

3. *Salmonella* infection of macrophages induces ADP-ribosylation of multiple host cell proteins.

We then moved from infecting HeLa 229 cells, epithelial cells, to macrophages from PMA-inducted differentiated monocytes. As immune cells, they play an important role in fighting bacterial infections.

Thus, we initially started using the gentamycin after 6 hours and collecting the sample in 2x Laemmli dye. We saw, when probing with the Af1521 (Figure 15A), a similar signal to the one previously seen with HeLa 229 cells, detected between 55 and 35 kDa, clearly visible from 12 hours onwards. Actin also showed a decrease of loading from infected samples when compared with control (Figure 15A). Additionally, a new host cell-specific signal is

visible from the second hour of infection with approximately 100 kDa. This signal increases intensity until 6 hours, after which, the signal is lost. Lastly, control samples from 24-hours' time point is overly intense, similar looking to H_2O_2-treated samples. However, as THP-1 untreated are suspension cells, clumps of cells may appear and justify an overcontent of protein, higher than other wells. This is also supported by the higher actin stain in the same lane.

Whereas, when probing with the polyclonal anti-PAR, we can see clearly the bacteria originated signals from 70 kDa and lower (Figure 15B). The new signal visible with the macro domain, here is also visible, although only from the third hour of infection. Curiously, two other bands extricate from the blot coming from host cell proteins. One is between 100 and 70 kDa also only clear after 3 hours of infection and lost after 12 hours. The other is at much lower weight with apparently only 15 kDa. This signal, however, is only visible at 5 and 6 hours.

Concluding from these results, we saw much more ADP-ribosylation activity in macrophage cells infected with *Salmonella* than in HeLa 229 cells with 3 new signals detected.

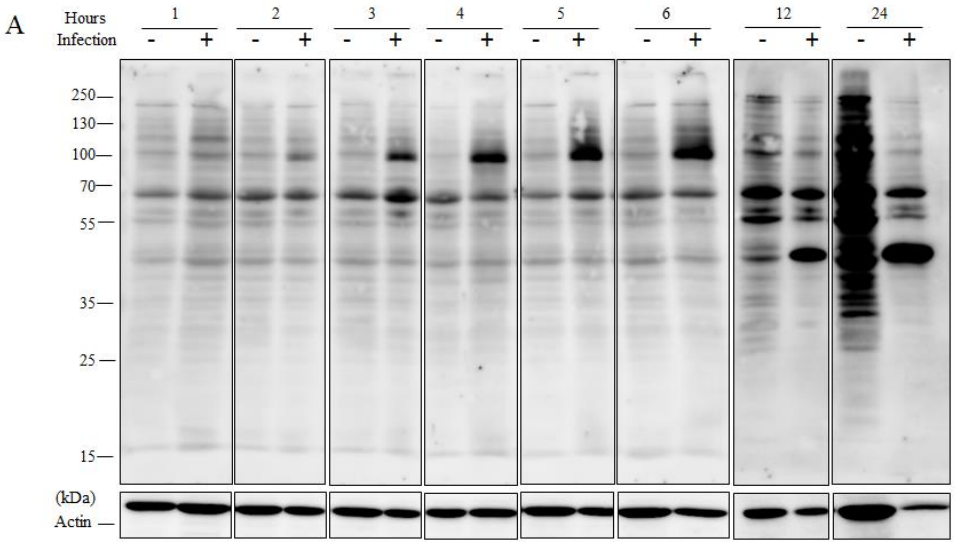

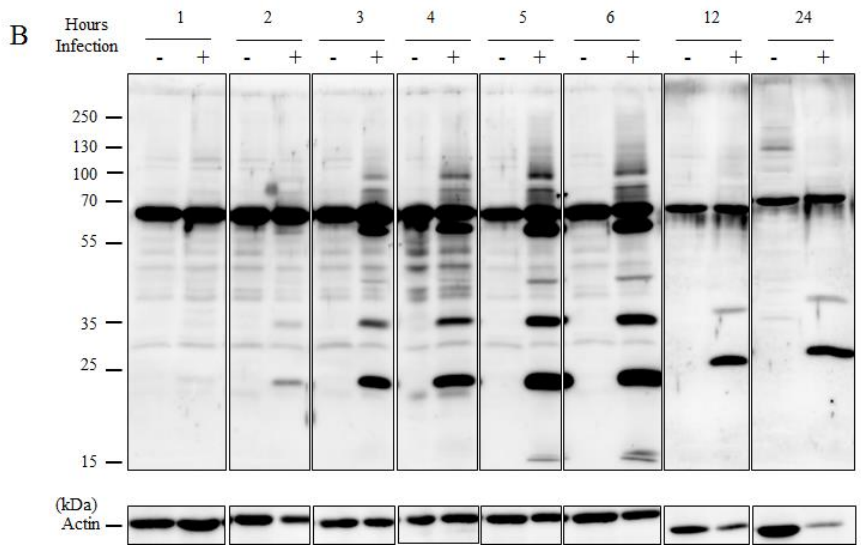

Figure 14 - THP-1 infection with *Salmonella* shows new and previously seen signals from both mono- and poly-ADP-ribosylation. THP-1 infected cells infected with *Salmonella*. Samples collected with 2x Laemmli dye. Probed with Af1521 and anti-GST (A) and polyclonal PAR (B).

a. Incubation of 1 hour before gentamycin addition is enough to induce modifications in THP-1 cells

Following, as to reduce signal from bacteria for it might be blocking signal that we would want to see but couldn't. Additionally, the growth of bacteria in 3 ml of media during 6 hours reaches such high volumes that it would overwhelm the cells and cause them to simply die rather the fight the infection. In literacy review for the method we saw that 1 hour of infection before gentamycin addition would be enough (Birmingham, Smith, Bakowski, Yoshimori, & Brumell, 2006; Valle & Guiney, 2005). So, we redid the experiment and used GAPDH as new control for the loading as actin could be compromised, however, we can see a gradual fading of this protein in infection-specific samples from hour 3 onwards until 12 hours when it seemed almost completely missing (Figure 16).

Then, when probed with polyclonal anti-PAR (Figure 16A), the fading of intensity from signals bacteria-specific when compared to the previous experiment. However, the new band at 100 kDa seems very strong at 2 and 3 hours, starting to fade at 4 hours, simultaneously as GAPDH and PARP14. Additional bands could be seen at 35 kDa, 25 kDa and the last one at 15 kDa.

Afterwards, when probed with the modified macrodomain Af1521 (Figure 16B), the only signals visible were the bands at 100 kDa, also seen with the polyclonal anti-PAR, already detectable at 1 hour, strongest and 2 and 3 hours of infection from then on, the signal starts to fade until at 12 hours where no signal can be noticeable. Additionally, the band between 55 and 35 kDa is also clear at 12 hours' time point.

As such, 1-hour incubation with bacteria is enough to cause modification in the THP-1 cells proteome and eliminates signals from bacterial proteins. Addition of gentamycin is now at 1 hour past adding the bacteria rather than 6 hours.

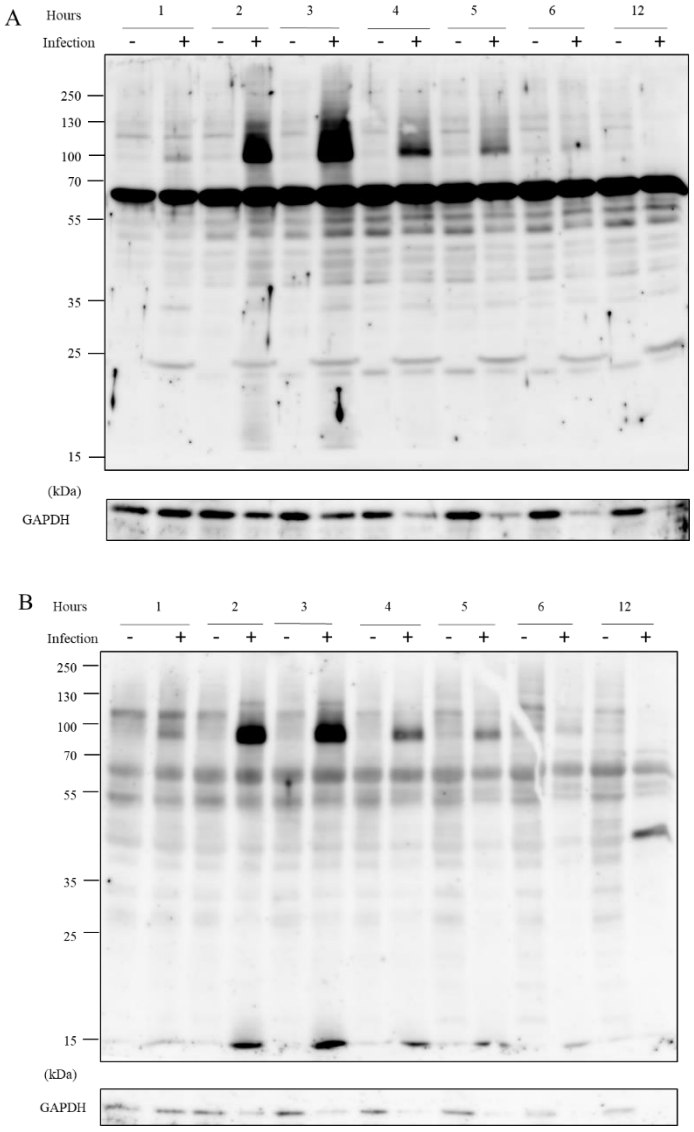

Figure 15 – Earlier addition of gentamycin in THP1 cells infected with *Salmonella* allowed for better detection of mono- and poly-ADP-ribosylated proteins. THP-1 with gentamycin after 1 hour. Samples collected with Laemmli dye. Probed with polyclonal anti-PAR (A), modified macrodomain Af1521 and monoclonal anti-GST (B) and polyclonal anti-GAPDH antibodies.

b. Variation in the addition of gentamycin led to no changes in HeLa 229 cells results

As we redid the experiment with the THP-1 cells trying to clear if the we could see better infection-specific results and actually concluded that 1 hour would be necessary for the infection for macrophages, we also redid with HeLa 229 cells. Here, we again used the actin as loading control and in the upper blot the loading seems good as all samples seem to have equal signal, whereas, in the lower blot actin signal at 24 hours infection time point the actin signal is lower than the remain samples.

As for ADP-ribose-specific signal, no signal was found related to poly-ADP-ribose residues as the membrane probed with polyclonal anti-PAR lacks any signal other than unspecific (Figure 17B). Additionally, the membrane probed with macrodomain Af1521 showed no other signal than the one between 55 and 35 kDa (Figure 17A).

Comparing these last two points we can see that there are similarities and differences between in ADP-ribosylation in macrophages epithelial cells infected with *Salmonella*. Both show a signal between 55 and 35 kDa, but while that is the only signal detected in HeLa 229 cells, THP-1 showed two others signals.

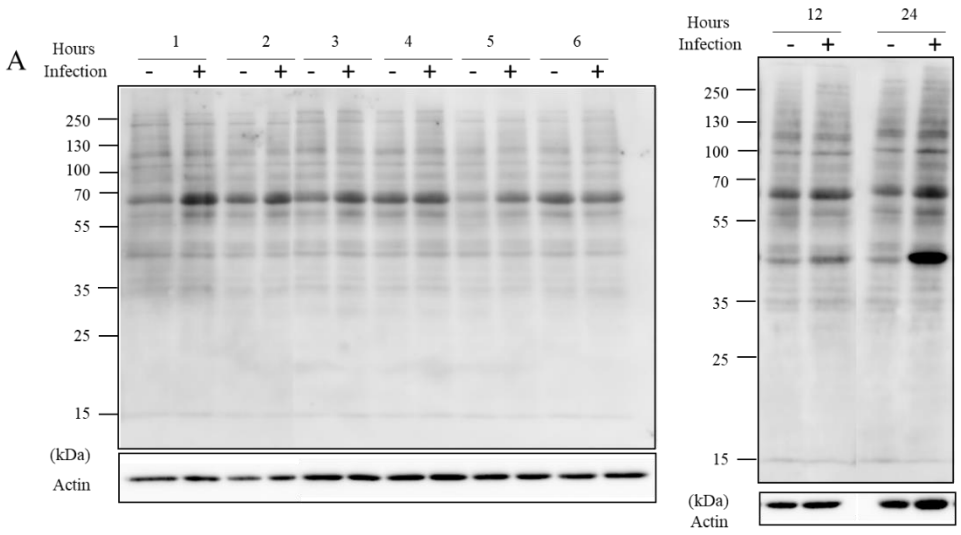

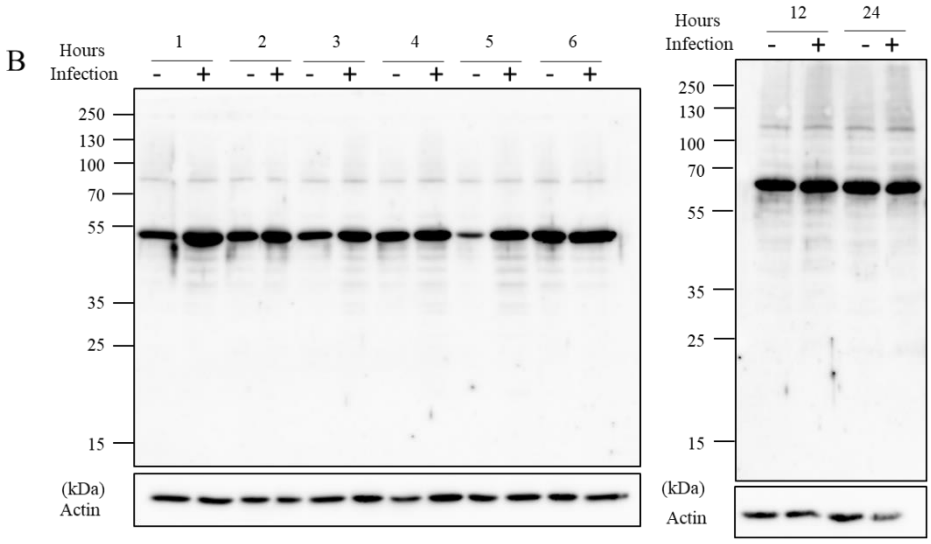

Figure 16 – *Salmonella* stimuli induced uniquely one mono-ADP-ribosylation in HeLa 229 cells. HeLa 229 cells infected with *Salmonella*. Gentamycin added after 1 hour. Samples collected with 2x Laemmli dye. Probed with macrodomain Af1521 and monoclonal anti-GST antibody (A) and with polyclonal anti-PAR (B) antibodies.

4. Buffy coat infection with *Salmonella* showed no infection-specific signal.

As the THP-1 cells showed infection-specific signals, we then moved to using cells originated from Buffy coat extraction as it contains leukocytes and platelets, among them the monocytes and macrophages. When probed with macrodomain all lanes look fairly the same with only one band visible in *Shigella* sample at 1 hour having a band at 35 kDa that on later time points is also visible (Figure 18A).

As when probed with the polyclonal anti-PAR antibody (Figure 18B) we saw, in *Shigella* infected samples, signal at 55 kDa, approximately 35 kDa and 15 kDa, which could be seen at any time point. In *Salmonella*-infected samples, we saw signal at 50 kDa and 25 kDa, starting at 3 hours, 35 kDa at 6 hours. These signals were the same as seen above corresponding to the bacterial lysates and not the cells-self proteins (Figure 13).

As such, infection of buffy coat-originated cells with *Salmonella* and *Shigella* produced no ADP-ribosylation-caused signal.

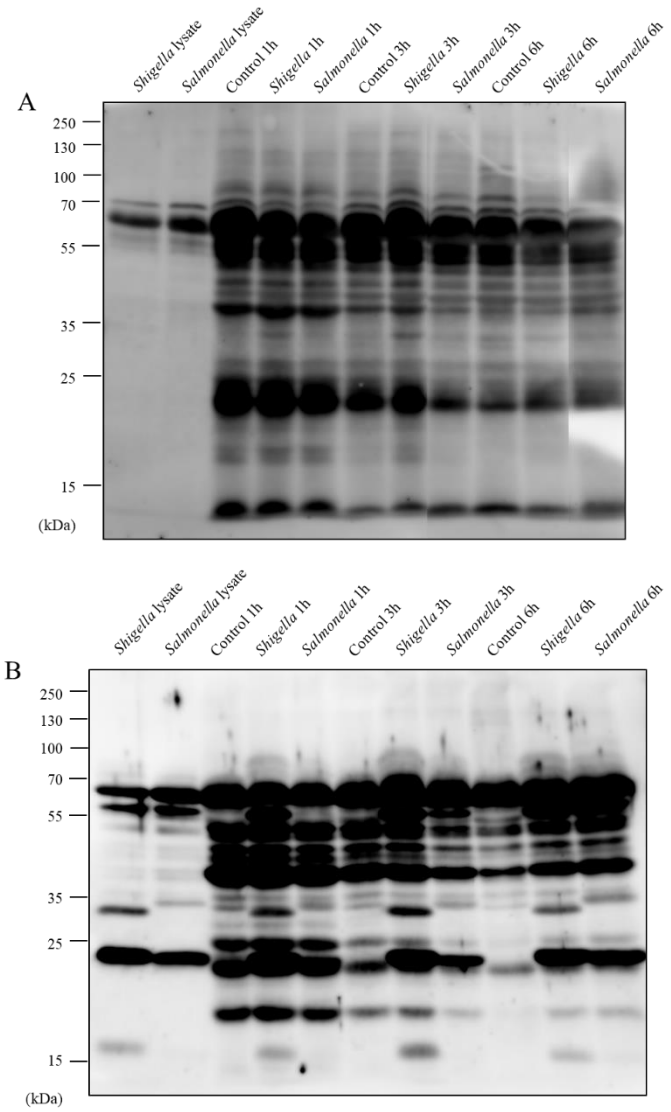

Figure 17 – No signal detected in infection of Buffy coat-originated cells. Buffy coat infection with *Shigella* and *Salmonella*. 1 and 2 are bacterial controls for *Shigella* and *Salmonella*, correspondingly, 3, 6 and 9 are controls; 4, 7 and 10 are *Shigella*-infected samples and 5, 8 and 11 are *Salmonella*-infected samples. 3-5 from 1-hour time point; 6-8 are from 3 hours' time point and 9-11 from 6 hours' time point. Sample collection done in Laemmli dye. Probed with modified macrodomain Af1521 and monoclonal anti-GST (A) and polyclonal anti-PAR (B) antibodies.

5. qPCR and Western blot for expression of PARP14 and PARP1 in infection with *Salmonella* and cytokine stimuli.

In Caprara et al., 2018, a role for PARP14 was studied relating its induction with inflammation. Using LPS, IFNβ and IFNγ as stimulates, cells expressed higher levels of

PARP14. Wondering now if this PARP could be also activated during bacterial infection, we assessed expression levels by qPCR as well as protein quantification by Western blot.

a. Bacteria and LPS and IFNγ induce changes in expression of *parp1* and *parp14* in HeLa 229 cells.

To assess whether PARPs expression was changed under stimuli by bacteria, LPS or cytokines, two initial PARPs were chosen: PARP1 and PARP14 based on their identified roles in cell biology. Starting with p*arp1* expression as it is the major ADP-ribosylating enzyme in the cells and (Figure 19).

What was seen under LPS and IFN incubation was at first 15 min, it remains unchanged. After 1 hour it is increased but not much higher than control at a 1.2-fold change. However, at 3 hours, it showed a 10.6-fold change. This effect is completely gone at 5 hours when it appears to have again the same values as control when taking the standard deviation into account.

As for *Salmonella* infected cells, these show a slight increase starting already at 15 min and lasting until 1 hour, when it reached the 2.3-fold change to the control values. After this time, the expression seems to start decrease. However big the start deviation is it, it remains lower than at 1 hours in both 5 hours and 12 hours. *Shigella*-infected samples show the same pattern, with an increase starting at 1 hour at 2-fold change, reaching higher than 3-fold change at 3 hours but, then, decreasing to values like control at 5- and 12-hours' time point.

In response to bacterial infection, cells demonstrated an initial response by increasing the expression of *parp1* whereas in response to stimuli from LPS and IFNγ, cells express one peak of *parp1* at 3 hours.

We see that in the initial hours all stimuli influenced *parp1* expression values.

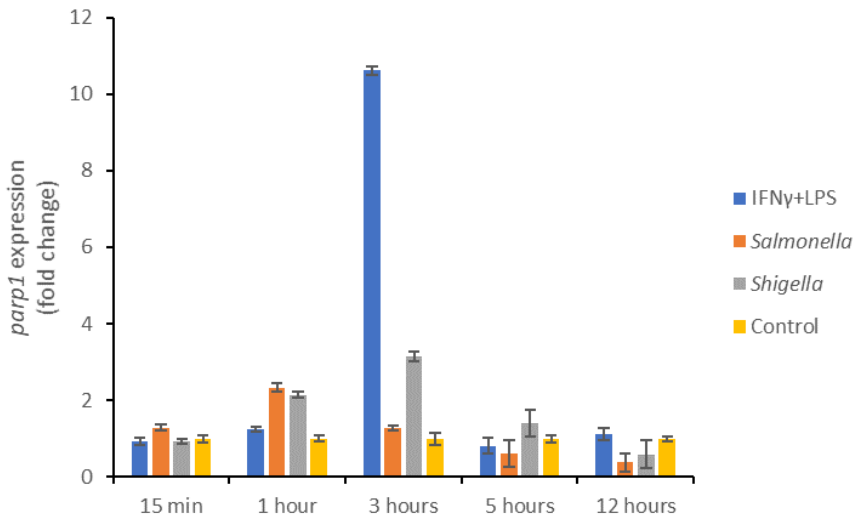

Figure 18 – Bacteria and LPS and IFNγ induce changes in *parp1* expression. *parp1* expression in untreated cells and treated with *Salmonella*, *Shigella* or IFN and LPS.

As for *parp14* expression (Figure 20) under IFN and LPS simultaneous stimuli was at the first hour lower than control samples, however, after 3 hours its expression rises from 6 times the expression in control to almost 8 times at 5 hours to end at 22 times higher after 24 hours incubation.

Under infection with *Salmonella*, it appears that *parp14* expression is lower at the first hour with almost a tenth of the expression in control samples. However, later, the values seem similar for 3 hours and 5 hours and the last results has too high standard deviation to take any conclusion.

The same can be said for *Shigella*-infected samples, where at 15 min and 1 hour, the expression values of parp14 are lower than in control samples with 0.4- and 0.17-times fold change, respectively.

Closing, comparing these results, we observe that under bacterial stimuli, while *parp1* is increased, *parp14* is decreased. As for LPS and IFNγ, together they lead to increase in both genes expression. These results, however, lack statistical analysis as no time was available to repeat the experiment times enough to be possible for analysis. As such, these results cannot be classified as significant but can point towards a possible outcome of what happens.

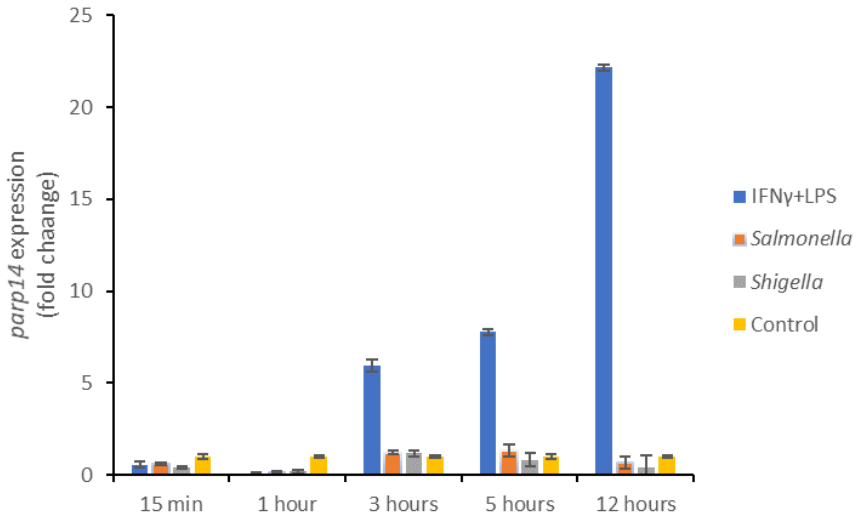

Figure 19 – LPS and IFNγ induce very high expression of *parp14*. *parp14* expression values in untreated conditions and treated with *Salmonella*, *Shigella* or IFN and LPS

b. Stimuli from bacteria, LPS or cytokines leads to differential expression of PARP1 and PARP14

Next, we wanted to see what happened, in protein levels, to the expression of PARP1 and PARP14 under stimuli from *Salmonella*, LPS or cytokines in HeLa 229 cells.

The samples from HeLa 229-cytokine stimulated were collected after trypsinized and lysed using NP-40 lysis buffer so that the protein concentration was known and equally loaded. For the most part, as we can see for the actin probing, we can see it to be true as most samples do have an equal amount of actin in all lanes. However, it appears uneven in some as for the first two hours of IFNα-treated samples (Figure 21B) and TNFα-treated samples (Figure 21D). The final time point of LPS-treated samples also appear to have more protein than the previous time points. Whereas the infected samples were collected in loading dye. Probed with GAPDH, we can see some samples lacking signal as control samples from 3 hours and all samples from 12 hours' time point (Figure 21E).

In samples incubated with IFNγ (Figure 21A), probing with anti-PARP1 shows a strong signal 24 hours prior cytokine addition. No other signal is visible. Whereas PARP14 probing shows a weak band present at 2-, 8-, 12- and 24-hours' time points in IFNγ positive samples.

As for IFNα (Figure 21B), PARP1 signal appears in control samples at 8 hours and 24 hours as well as in cytokine-incubated samples only at 24 and 48-hours' time points. PARP14 bands started to be clear at 12 hours and last until 48 hours in after IFNα stimuli.

PARP1 expression after LPS expression is increased in later time points – 24- and 48-hours' time point, while in TNFα-stimuli (Figure 21D), its expression is increased in the first 2 and 8 hours. Neither of these two cytokines seemed to have any affect in PARP14 production as no signal is visible.

As for HeLa cells infected with *Salmonella* (Figure 21E), the infection seemed to have no effect in PARP1 expression as its signal from samples from 2 to 24 hours seemed the same. As for PARP14 the initial signal seemed higher than later time points, however no difference was seen between infected and non-infected samples. However, all these variations could be explained by the different amounts of loading as the PARP14 expression is in tune with GAPDH's.

Concluding, in epithelial cells, PARP1 expression is changed under influence of cytokynes but not by *Salmonella* infection, whereas, PARP14 expression is changed under influence of interferons and *Salmonella* infection but not by LPS and TNFα.

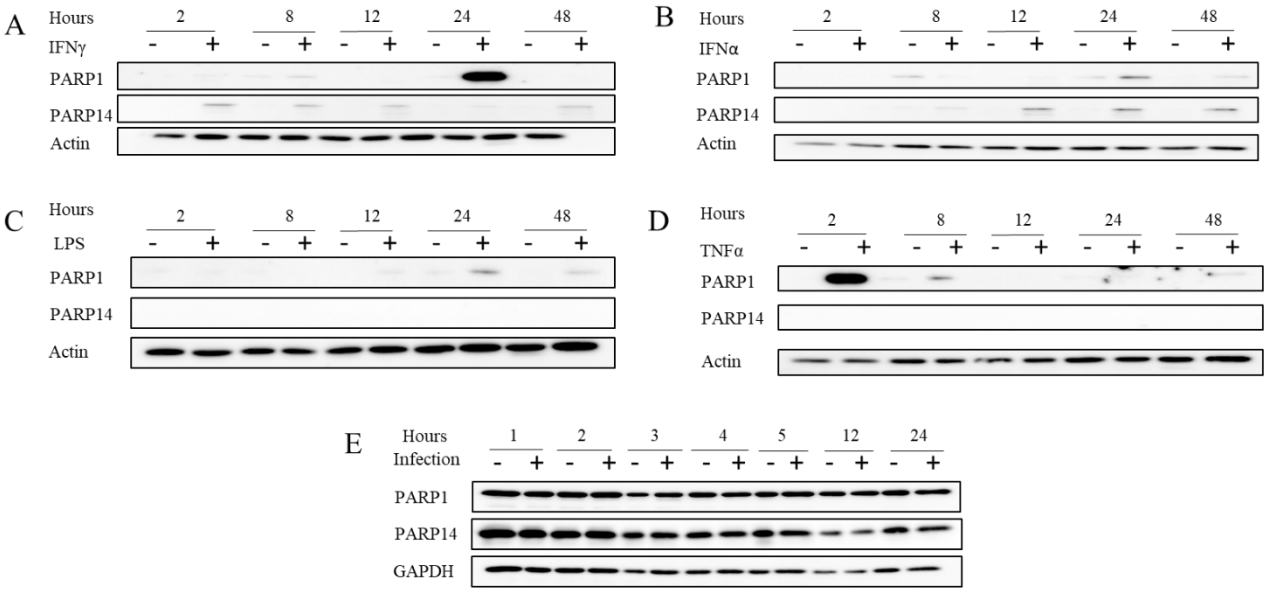

Figure 20 – PARP14 and PARP1 expression in HeLa 229 cells varies with stimuli. PARP14, PARP1 and actin expression levels in Hela 229 after stimuli with cytokines (A, B and D) and LPS (C) and after incubation with *Salmonella* (E) with gentamycin after 1 hour. Samples collected by trypsinization. Probed with monoclonal anti-PARP1 and anti-PARP14 antibodies.

c. THP-1 expression of PARP1 and PARP14 after stimuli from *Salmonella*, LPS or cytokines

Following is the same study of PARP1 and PARP14 in THP-1 differentiated with PMA to macrophages. This time we additionally probed for ICAM1 whose expression is increased in response to TNFα stimuli, which in turn is produced in response of LPS presence. Such is verified on the lanes containing LPS- and TNFα-stimulated cells (Figures 22C-D). As such, in those samples, namely, 24 and 48 hours for the former and 8, 24 and 48 hours for latter, ICAM 1 signal is higher when compared to control samples. The loading in cytokine-stimulated samples appears equal except for the lane with IFNγ-stimulated cells for 48 hours and the samples from infection with *Salmonella*. These samples were collected with loading dye which would explain the uneven loading.

As for the PARP1 signal after IFNγ incubation (Figure 22A), it is visible at 12 and 24 hours in a very faint band. Whereas the PARP14 are clear at 8, 12 and 24 hours with some intensity. This band, however, is not present at 48 hours incubation time point, however this the exact sample with lower actin signal so it might be that the protein concentration was not enough to see the signal.

Curiously, IFNα seemed to the same effect on both PARP1 and PARP14, as both bands show at 8 hours and last until the last time point (Figure 22B). PARP1 seemed unresponsive to LPS-stimuli (Figure 22C), however, PARP14 band shows grows from 8 hours lane to 48 hours. The last cytokine, TNFα, has a peak in PARP1 protein production (Figure 22D) as an only band is visible at 8 hours and then it's gone. PARP14, in the other hand has no clear expression at any of the time points.

Lastly, in *Salmonella*-infected cells (Figure 22E), no observation scan be done for the last two time points as actin shows very uneven signal between control and infected samples. However, when looking at earlier time points, a decrease in PARP1 is seen at 4 hours as well as 6 hours as for infected samples. PARP14 shows a roller-coaster of intensity as at the first hour it seems stronger, then at 2 hours onwards, it is lower. However, it also varies within control samples, as at 4 hours it shows a lower signal while all other samples look in tandem with the loading control.

To conclude from this result as well, in macrophages, PARP1 expression is altered under stimuli from the cytokines and *Salmonella* infection but not by LPS-stimuli. As for PARP14

both interferons, LPS and *Salmonella* infection lead to changes in its expression while TNFα does not.

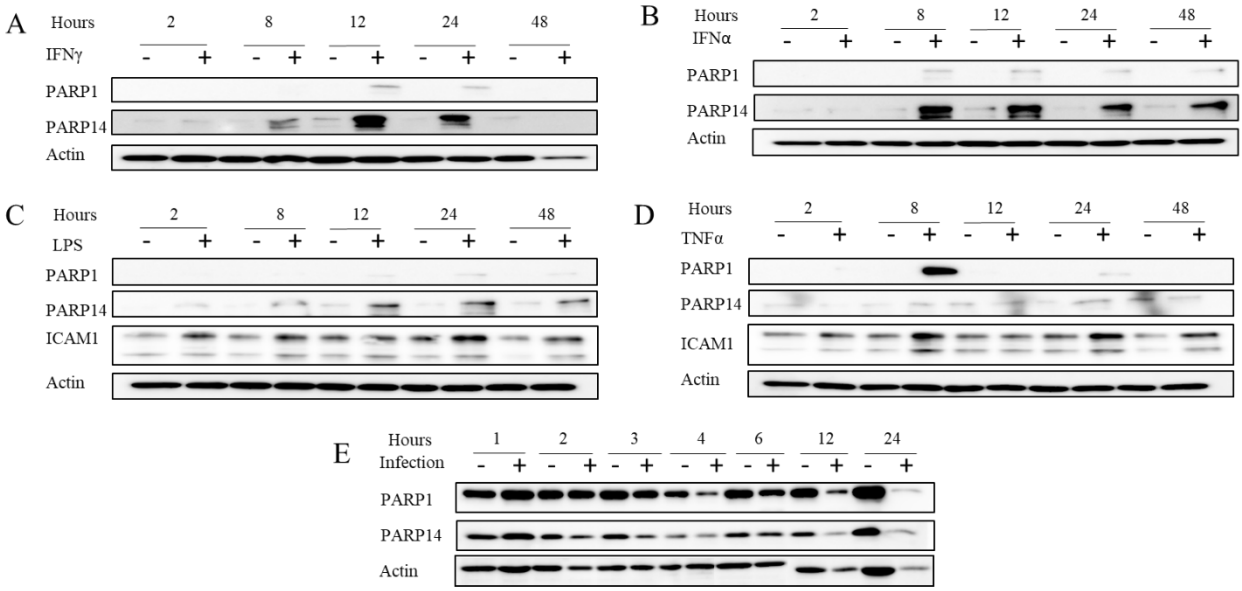

Figure 21 – THP-1 differential expression of PARP1 and PARP14 after stimuli from bacteria, LPS or cytokines. PARP14, PARP1 and actin expression levels in THP-1 PMA-differentiated after stimuli with cytokines (A, B and D) and LPS (C) and after incubation with *Salmonella* (E) with gentamycin after 1 hour. Samples collection by trypsinization. Probed with monoclonal anti-PARP1, anti-PARP14 and anti-ICAM1 antibodies.

6. ADP-ribosylation in response to cytokine treatment

For the last result, we wanted to see if the cytokines had any influence in the whole ADP-ribosylated protein profile. As such, we incubated PMA-differentiated macrophages with the same cytokines and at specific time points, collected samples with 2x Laemmli dye.

Loading control was done with actin as it should remain constant despite cytokine incubation. That is verified by the uniformity of the actin bands in all blots.

When probing with polyclonal anti-PAR (Figure 23), only band shows that is not present in control samples, that is a band at 100 kDa in response to LPS stimuli. This band shows at 2 hours and does not appear in other time points. However, a band seemly this same size is also visible in the membrane probed with the modified macrodomain (Figure 24).

Under this probing, samples from IFNγ, IFNα and TNFα, have no different bands from control nor the other way around. LPS, on the other side, besides the band mentioned above

shows two other bands, the first at nearly 130 kDa and the second approximately 15 kDa. All these bands show uniquely at 2 hours' time point.

To conclude our results, we demonstrated that only LPS induced ADP-ribosylation in a single protein.

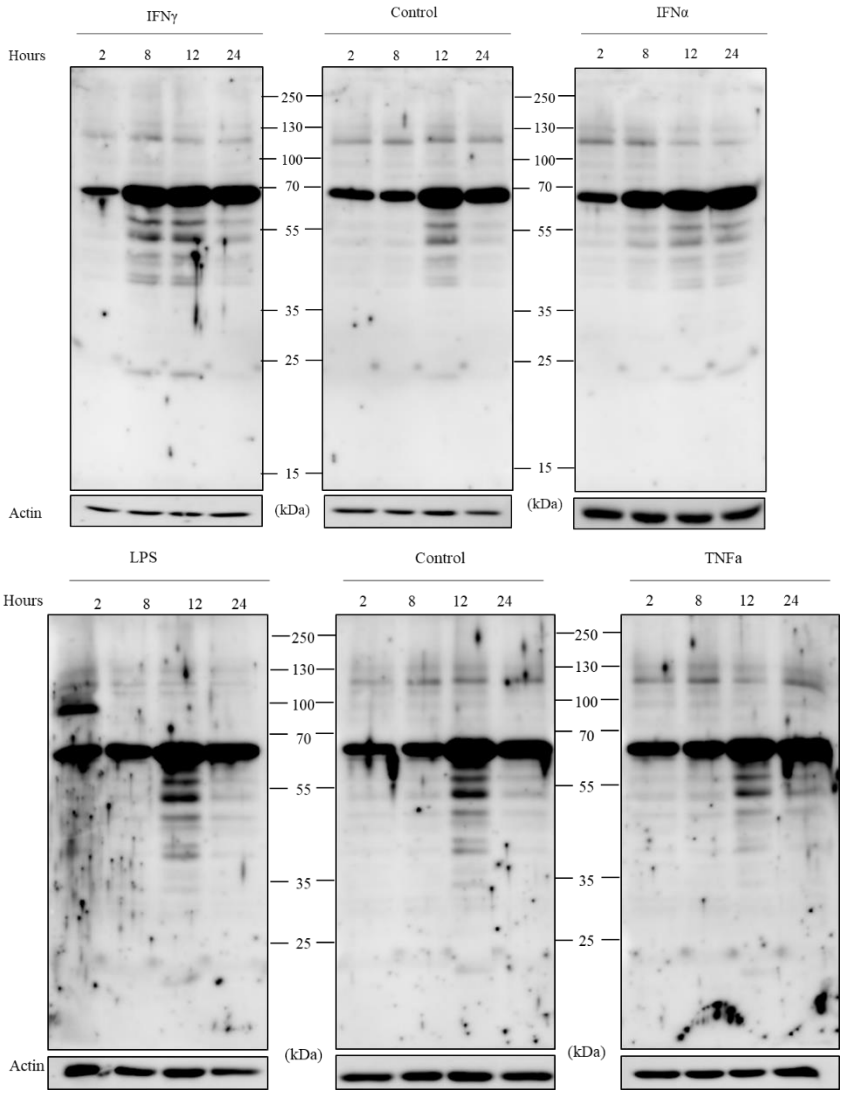

Figure 22 – LPS induces poly-ADP-ribosylation in THP-1 cells at 2 hours. THP-1 cells treated with cytokines or LPS. Samples collected in loading dye. Probed with polyclonal anti-PAR antibody.

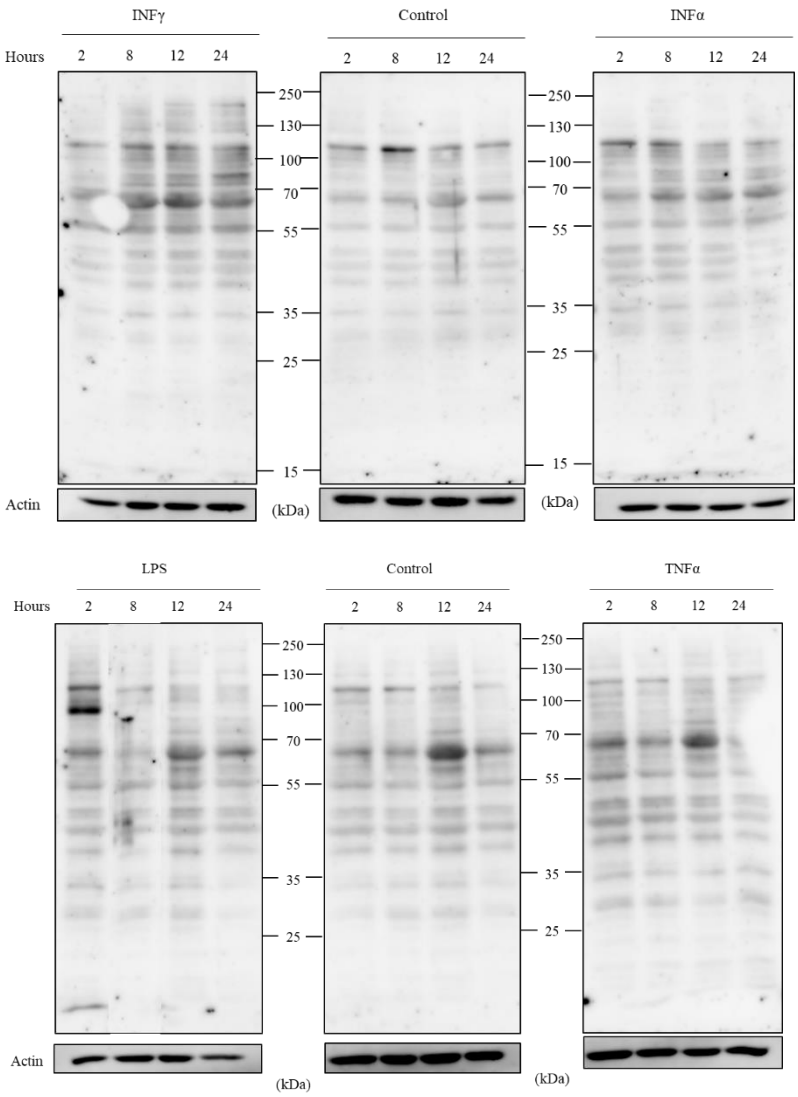

Figure 23 – Detect signal in THP-1 cells after LPS stimuli. THP-1 cells differentiated to macrophages treated with cytokines or LPS. Samples collected in loading dye. Probed with modified Af1521 and monoclonal anti-GST antibody.

Chapter IV – Discussion

ADP-ribosylation is an ancient post-translational modification present throughout the kingdoms of life. Bacteria uses it as a mechanism for pathogenicity and in eukaryotes it was demonstrated to have a varied range of functions. As more and more studies correlate ADP-ribosylation to stress responses, a role of this modification in bacterial infection seems likely. We set out to demonstrate that endogenous ADP-ribosylation is active during bacterial infection in human cells. To do that we had two main aims: detect ADP-ribosylated proteins in infected, LPS- or cytokine-treated epithelial cells and macrophage and quantify expression levels of PARPs in these same cells.

1. Epithelial cells infection successfully set up and visualized by flow cytometry.

As to try and assess the efficiency of infection, a method based on flow cytometry was drawn where *Salmonella* would be transformed to constitutively express GFP protein and as such be detected in a flow cytometer. The method was successful as seen in Figure 3A and 3B, where GFP-expressing *Salmonella* is clearly distinguished from WT *Salmonella*. On the next step for the goal to set up this method, it was tested if when incubated with cells, if the bacteria could reach and infected them. Furthermore, it tested if bacteria-associated cells would be detected in flow cytometry. Such was seen (Figure 4) as cells were washed before collection and thus non-cell-associated bacteria would be washed away. Differences between control and infected samples show the development of the infection as time passes.

ADP-ribosylation is a post-translational modification that much of its activity is related to stress, it was relevant to prevent any more stress to the cells, and it was tested if the removal of FBS would in any way affect the infection progression. It was seen that it seemly helped the infection as non-supplemented samples had higher percentage of bacteria-associated cells. However, after 4 hours, the effect is lost for *Salmonella* (Figure 4C and 5C), as from time point, the difference between invert.

Additionally, as the interest laid on cellular part of fighting infection, gentamycin is needed to be added to kill extracellular microbes. As such, the timing of the addition of antibiotic is important so that the bacteria had time to infect the cells but overpopulate the plate, as it causes extra stress to the cells, other than the infection itself. Some papers refer 1 hour or less as enough time however, as seen in Figures 4 and 5, such time is not enough for

differences to be detected in flow cytometry-based assay (Birmingham et al., 2006; Valle & Guiney, 2005).

However, a high signal from bacteria in flow cytometry assay might not be significantly enough but at a protein level could be enough to have a signal. While this assay would be interesting to use for the assessment of the infection evolution in medias supplemented with PARP and PARG inhibitors and gentamycin addition of gentamycin on a later time point, such could not be done as there was not enough time.

A another point worth mention is the lack of repetition. These assays were only performed once each and in different conditions, so no statistical analysis is available, however, both results are clear of their meaning.

2. Bacterial infection induces ADP-ribosylational changes to epithelial cells

Next, as it was hypothesised that ADP-ribosylation had a role during *Salmonella* infection, as such, samples from *Salmonella* infection and control were run for Western-blot and later probed for ADP-ribosylation. Initially, this infection protocol was set up with HeLa 229 cells and collection with modified RIPA buffer containing PARP and PARG inhibitor as to avoid any loss of signal (Figures 6-9). Af1521 macrodomain is "reader" for ADP-ribose moieties bond to proteins, either those are mono- or poly-ADPR. Modified to contain a GST in its structure by using an anti-GST antibody we can detect and visualize the PTM. The only residue clear in HeLa cells was a signal between 35 and 55 kDa present in *Salmonella* infected-samples (Figure 7). This same signal was not seen when probing with polyclonal anti-PAR, which can only detect poly-ADP-ribosylation, as such we would speculate that this protein is only being mono-ADP-ribosylated. In the literature review, it is mentioned the existence of an effector protein capable of ADP-ribosylating actin and the resulting protein has an approximate size of 45 kDa. As, so far, bacteria have only been showed to be able to mono-ADP-ribosylate its targets, it would appear that the signal showed is this ADP-ribosylated actin. Furthermore, actin probing in later time points show a weakening of actin signal (Figure 12G). This could also be explained by, as the infection progresses, more cells die and as such, so does the actin content. However, no proper identification method was done and many other proteins in the HeLa 229 cells could fit the estimated size. This signal appears to be only present after 12 hours of infection.

When probing with polyclonal anti-PAR antibody the first lane profile of a sample from *Shigella*-infected cells showed multiple signals at 55, 35 and 25 kDa. While, *Salmonella*-infected samples showed three bands at similar sizes, which were initially suspected of being poly-ADP-ribosylated proteins (Figure 8 and 9).

Later, it was done the same infection set up, but the media was supplemented with Rucaparib, a PARP inhibitor, to assess if these same bands were still present. The results show the same bands unaltered (Figure 12). This result brings doubts about the origin of these signals, whether they could truly be ADP-ribosylated proteins and if they are even truly originated from the cells proteins. Additionally, the fact that these signals are not present when probing for the macrodomain Af1521, when it should detect both mono- and poly-ADP-ribosylated proteins questions the origins of these bands. So, next the original experiment was redone and added a new control in which only bacteria would be present ion order to differentiate between bacteria-generated signal and infection specific signal. In here, it was showed how all the signals previously seen came from bacteria rather than from cells (Figure 13). This conclusion is also supported by the results when gentamycin was added after 1 hours as no signal was seen. The exception would be the signal previously seen between 35 and 55 kDa which was also lacking from bacteria lysate but present in infection samples, demonstrated it come from cell in the course of the infection (Figure 13C).

Now, as these signals come from bacteria, the question is if they truly are ADP-ribose or could it be the antibody binding to unspecific proteins present in the bacteria lysate, as in all the antibodies bond to signals coming from *Shigella* and *Salmonella*, both monoclonal and polyclonal.

Of the methods available to remove ADP-ribose moieties from proteins, they are all dependent of the type of amino acid to which the ADP-ribose is bond to. Treatment with Hydroxylamine has been showed to be able to remove residues bond to acidic amino acids. The treatment of this molecule in bacterial lysates again showed no effect in the presence of these bands (Figure 14). If did have an effect it could mean that they are poly-ADP bond to aspartate or glutamate, as it did not, they are either bond to some other amino acid or they can be unspecific bind to some proteins in bacterial lysates. Additionally, it could also mean in the bacteria there are enzymes capable of poly-ADP, which has not been identified yet.

Curiously, in these samples, both samples look the same, with no difference between *Salmonella* and *Shigella* lysates with many of signal seen previously lacking. However, the origin of these protein bands would have to be further investigated.

To conclude, in HeLa 229 cells infected with *Shigella* and *Salmonella*, it was only seen a band corresponding a 35-55 kDa protein which is mono-ADP-ribosylated in *Salmonella*-infection and any other signal is irrelevant to the role of the endogenous ADP-ribosylation in infection by bacteria. The assay conducted with gentamycin after one hour supports this claim (Figure 17).

3. Macrophages demonstrate higher ADP-ribosylation activity during *Salmonella* infection

Ensuing, the direction of the work was moved towards immune cells implicated in the response to bacterial infection as macrophages are. THP-1 differentiated to macrophages by PMA action substituted the HeLa 229 cells. Following the same infection set up, Western-blotting these samples targeted to *Salmonella* infection solely. Probing with the macrodomain Af1521 demonstrated the presence of the same band as the one present in HeLa 229 infected cells and an additional one at 100 kDa, the latter was also visible in blots probed with polyclonal anti-PAR, suggesting it to be a signal from a poly-ADP-ribosylated protein (Figure 15). This signal, however, is a faster response to the infection as it shows after only 2 hours of incubation with *Salmonella* and at 12 hours is gone. Two other signals are present when probed with polyclonal anti-PAR antibody, one a bit higher than 70 kDa which shows the same pattern as the previous discussed signal, and a smaller one at 15 kDa (Figure 15B). None of the three signals were present in HeLa 229 infected cells.

When infection was done in which the gentamycin was added after 1 hour, a much clearer blot was seen in which almost all signal from bacteria is gone and the infection-specific signal was clearer (Figure 16). This time it was possible to see the band between 35 and 55 kDa, the one at 100 kDa and the one at 15 kDa. These latter ones were present in both blots and as such propose poly-ADP-ribosylation in both while the former remains as mono-ADP-ribosylated. Unfortunately, this method does not specify the origin of the modifying agent meaning that it is unknown whether the cell itself caused this modification or the bacteria, however, no poly-ADP-ribosylation from bacteria has been reported indicating a endogenous function.

As a it is made of the immune cells present in the blood, it was expected to see similar looking results with Buffy coat cells. However, no signal was seen with the infection with *Salmonella* (Figure 18). This result could be explained by low numbers of macrophages in blood as well as possible contamination by red blood cells making the cell count wrong towards the number of white cells present. *Shigella*-infected cells yielded similar results with no signal being infection-specific but rather just bacterial-specific (Figure 18).

4. Bacteria, LPS and cytokines induce changes in expression of PARPs in epithelial and macrophages cells

PARPs were corelated to inflammation in murines macrophages as well as to hinder *Salmonella Typhimurium* proliferation (Caprara et al., 2018). It was to our interest to also test in human endotherlial cells and macrophages the expression of PARP1 and PARP14 under inflammatory cytokines as well as LPS. As the main PARP active in the cells, PARP1 is the main suspect when assessing for ADP-ribosylation. PARP14 on the other hand as been identified to be to have a role in IFN response (Caprara et al., 2018).

With that goal in mind, the analysis for these PARPs had two approaches, an initial one by qPCR in which HeLa 229 cells were tested against *Salmonella*, *Shigella* and IFNγ and LPS combined. The same assay preformed with THP-1 cells unfortunately would be beyond the time available. The second approach was based on western blotting for PARP1 and PAR14 in HeLa 229 and THP-1 cells after incubation up to 48 hours with the cytokines or LPS.

In HeLa 229 cells, PARP1 overexpression appeared after IFNγ and TNFα-stimuli, however at very different time points, 24 hours for the former and 2 for the latter (Figure 21A-D). Interesting, LPS incubation did not increase PARP1 expression in an intense manner (Figure 21C). The use of LPS and IFNγ together in quantitative expression analysis had two purposes, the first was to serve as a positive control as showed (Caprara et al., 2018) that either would lead to an increase in *parp14* expression in murine cells. The second and main one was to also see the pattern it would follow the *parp14* expression in HeLa 229 cells. When looking at the expression of *parp1*, we see a peak at 3 hours under IFNγ and LPS simultaneous signal (Figure 19).

In these cells, PARP14 had an overall low expression in all situations, it was completely lacking any signal after LPS- and TNFα-treatment and was detected at very low levels in the interferons containing samples. IFNγ-effect showed to happen in the earlier time points while IFNα acts on a later time point (Figures 21A-B). Meaning that, in response to the

interferons, PARP14 is also getting up-regulated in HeLa 229 cells. However, on *parp14* expression it was seen a clear increase up to 20-fold change in response to LPS and IFNγ at 12 hours (Figure 20). Based on the results seen here, we see, based on gene expression, although PARP14 protein amount should be increasing, in protein content the amount is reducing. This could mean that there is a mechanism cutting off the increase of protein between transcription and translation. As LPS stimulated cells showed no amount of PARP14 at all, it is assumed that the effect in *parp14* is due only to IFNγ stimuli or, rather, the combined effect of LPS and the interferon lead to an exacerbated expression of parp14.

Salmonella infection had no effect in PARP1 and PARP14 expression in HeLa 229 cells (Figure 21E). While LPS had an increase of PARP1 at 24 hours, matching the time for its effect to happen in the cells, the same could not be seen in the *Salmonella*-infected cells (Figures 21C and 21E).

As for THP-1 cells, although lacking the mRNA expression levels and solely based on the Western-blot results, a similar profile in seen for the PARP1 expression, meaning that this PARP1 activation is not cell type-dependent in the response to IFNα, LPS and TNFα, although the big signal present in the last shows later than the 2 hours and instead is only visible at 8 hours (Figure 22). However, PARP1 is known to auto-ADP-ribosylate in self when active, so the lack of signal when searching for the modification at the expected size of the enzyme questions what role the increase in the cells plays. As for IFNγ the strong signal present at 24 hours, meaning that this response is cell type-dependent.

PARP14, also keeps the same pattern as seen in HeLa cells, although the increase of signal in IFNγ did show later but was also gone by the 24 hours Figure 22A). TNFα again shows no specific effect in PARP14 signal (Figure 22D).

LPS, in the other hand, shows a very different profile compared to Hela 229 cells. In THP-1 cells, a signal shows already 2 hours and lasts for the duration of the 48 hours (Figure 22C). However, the same could not be seen in *Salmonella* infected samples (Figure 22E) as in these there is no increased signal in the samples at any time point. *Salmonella* infection only seem to cause a decrease in PARP1 at 4- and 6-hours' time point. After that, no conclusions can be done as loading is uneven.

5. LPS induces ADP-ribosylation in macrophages

As HeLa 229 showed weak signals, the search for ADP-ribosylation as response to LPS and the cytokines was only preformed in THP-1 cells. In those it was seen that no cytokine showed sign to induce the ADP-ribosylation of any protein (Figures 23 and 24). LPS however, presented a signal at 2 hours, around 100 kDa and another at 15 kDa, the first is present in both polyclonal anti-PAR and macrodomain AF1521, suggesting poly-ADP-ribosylation and the second only present in the macrodomain. The signals are similar looking to those present in *Salmonella* infection in the same cell type which would propose that LPS and *Salmonella* cellular response acts by ADP-ribosylation the same proteins.

Nevertheless, the signal between 55 and 35 kDa, is lacking in LPS-stimulated but is present in both cell types, meaning that this signal is unique to *Salmonella*-infection and cell-type independent.

Conclusions

ADP-ribosylation is a post-translational modification whose role in stress response is gradually increasing. Its association with inflammation and virus infection has already been seen (Gupte et al., 2017). Bacterial toxins were the first to show the PTM and many studies have already been based on it. On the other hand, cell-related functions have also been increasing. However, the study of the endogenous ADP-ribosylation in bacterial infections have only recently began.

In this work, using Western blot-based assays, ADP-ribosylation activity was detected in both human epithelial cell and macrophages and demonstrated to be active as well in *Salmonella*-infection. Multiple infection-specific signals were detected in both epithelial cells and macrophages in a cell type independent- and dependent-manner. The ADP-ribosylation seemed to be more present in macrophages indicating a more active role in immunity. Moreover, one of signals seen in macrophages was also detected after LPS-stimuli.

Additionally, it was assessed whether stimuli of bacteria, cytokines or LPS had any influence on the level of PARPs in epithelial cells and macrophages by Western blotting and quantitative PCR. In epithelial cells, cytokines- or LPS-stimulation both led to changes in the levels of PARP1, whereas infection by Salmonella had no effect. As for PARP14, in these cells, was unresponsive to LPS and TNFα but, in response to Salmonella and interferon, had its expression changed. Additionally, incubation with LPS and IFNγ led to an substantial increase of *parp14* expression. In macrophages, PARP1 and PARP14 expression had no changes in response to LPS or TNFα, respectively, whereas, stimuli by Salmonella and the remaining cytokines led the changes in these PARPs expression.

Concluding, this work contributes to the identification of cellular functions in which ADP-ribosylation is involved as well as elucidate on the events occurring during bacterial infection.

References

Agbor, T. A., & Mccormick, B. A. (2011). Salmonella effectors: Important players modulating host cell function during infection. *Cellular Microbiology*, *13*(12), 1858–1869. https://doi.org/10.1111/j.1462-5822.2011.01701.x

Aravind, L., Zhang, D., de Souza, R. F., Anand, S., & Iyer, L. M. (2014). The Natural History of ADP-Ribosyltransferases and the ADP-Ribosylation System. In *Life Science Journal* (Vol. 6, pp. 3–32). https://doi.org/10.1007/82_2014_414

Bai, P. (2015). Biology of Poly(ADP-Ribose) Polymerases: The Factotums of Cell Maintenance. *Molecular Cell*, *58*(6), 947–958. https://doi.org/10.1016/j.molcel.2015.01.034

Barbarulo, A., Iansante, V., Chaidos, A., Naresh, K., Rahemtulla, A., Franzoso, G., … Bubici, C. (2013). Poly(ADP-ribose) polymerase family member 14 (PARP14) is a novel effector of the JNK2-dependent pro-survival signal in multiple myeloma. *Oncogene*, *32*(36), 4231–4242. https://doi.org/10.1038/onc.2012.448

Barthel, M., Hapfelmeier, S., Quintanilla-Martínez, L., Kremer, M., Rohde, M., Hogardt, M., … Hardt, W. D. (2003). Pretreatment of mice with streptomycin provides a Salmonella enterica serovar Typhimurium colitis model that allows analysis of both pathogen and host. *Infection and Immunity*, *71*(5), 2839–2858. https://doi.org/10.1128/IAI.71.5.2839-2858.2003

Bartolomei, G., Leutert, M., Manzo, M., Baubec, T., & Hottiger, M. O. (2016). Analysis of Chromatin ADP-Ribosylation at the Genome-wide Level and at Specific Loci by ADPr-ChAP. *Molecular Cell*, *61*(3), 474–485. https://doi.org/10.1016/j.molcel.2015.12.025

Birmingham, C. L., Smith, A. C., Bakowski, M. A., Yoshimori, T., & Brumell, J. H. (2006). Autophagy controls Salmonella infection in response to damage to the Salmonella-containing vacuole. *Journal of Biological Chemistry*, *281*(16), 11374–11383. https://doi.org/10.1074/jbc.M509157200

Blériot, C., & Lecuit, M. (2016). The interplay between regulated necrosis and bacterial infection. *Cellular and Molecular Life Sciences*, *73*(11–12), 2369–2378. https://doi.org/10.1007/s00018-016-2206-1

Caprara, G., Prosperini, E., Piccolo, V., Sigismondo, G., Melacarne, A., Cuomo, A., … Natoli, G. (2018). PARP14 Controls the Nuclear Accumulation of a Subset of Type I IFN–Inducible Proteins. *The Journal of Immunology*, ji1701117. https://doi.org/10.4049/jimmunol.1701117

Cohen, M. S., & Chang, P. (2018). Insights into the biogenesis, function, and regulation of ADP-ribosylation. *Nature Chemical Biology*, *14*(3), 236–243. https://doi.org/10.1038/nchembio.2568

David, K. K. (2009). Parthanatos, a messenger of death. *Frontiers in Bioscience, Volume*(14), 1116. https://doi.org/10.2741/3297

Fàbrega, A., & Vila, J. (2013). Salmonella enterica serovar Typhimurium skills to succeed in the host: Virulence and regulation. *Clinical Microbiology Reviews*, *26*(2), 308–341. https://doi.org/10.1128/CMR.00066-12

Grady, S. L., Hwang, J., Vastag, L., Rabinowitz, J. D., & Shenk, T. (2012). Herpes Simplex Virus 1 Infection Activates Poly(ADP-Ribose) Polymerase and Triggers the Degradation of Poly(ADP-Ribose) Glycohydrolase. *Journal of Virology*, *86*(15), 8259–8268. https://doi.org/10.1128/JVI.00495-12

Gupte, R., Liu, Z., & Kraus, W. L. (2017). Parps and adp-ribosylation: Recent advances linking molecular functions to biological outcomes. *Genes and Development*, *31*(2), 101–126. https://doi.org/10.1101/gad.291518.116

Hottiger, M. O., Hassa, P. O., Lüscher, B., Schüler, H., & Koch-Nolte, F. (2010). Toward a unified nomenclature for mammalian ADP-ribosyltransferases. *Trends in Biochemical Sciences*, *35*(4), 208–219. https://doi.org/10.1016/j.tibs.2009.12.003

Iwata, H., Goettsch, C., Sharma, A., Ricchiuto, P., Goh, W. W. Bin, Halu, A., … Aikawa, M. (2016). PARP9 and PARP14 cross-regulate macrophage activation via STAT1 ADP-ribosylation. *Nature Communications*, *7*. https://doi.org/10.1038/ncomms12849

Kim, M. Y., Zhang, T., & Kraus, W. L. (2005). Poly(ADP-ribosyl)ation by PARP-1: `PAR-laying' NAD+ into a nuclear signal. *Genes & Development*, *19*(17), 1951–1967. https://doi.org/10.1101/gad.1331805

Kotewicz, K. M., Ramabhadran, V., Sjoblom, N., Vogel, J. P., Haenssler, E., Zhang, M., … Isberg, R. R. (2017). A Single Legionella Effector Catalyzes a Multistep Ubiquitination

Pathway to Rearrange Tubular Endoplasmic Reticulum for Replication. *Cell Host and Microbe*, *21*(2), 169–181. https://doi.org/10.1016/j.chom.2016.12.007

Kraus, W. L. (2015). PARPs and ADP-Ribosylation: 50 Years . . . and Counting. *Molecular Cell*, *58*(6), 902–910. https://doi.org/10.1016/j.molcel.2015.06.006

Langelier, M. F., Riccio, A. A., & Pascal, J. M. (2014). PARP-2 and PARP-3 are selectively activated by 5' phosphorylated DNA breaks through an allosteric regulatory mechanism shared with PARP-1. *Nucleic Acids Research*, *42*(12), 7762–7775. https://doi.org/10.1093/nar/gku474

Lesnick, M. L., Reiner, N. E., Fierer, J., & Guiney, D. G. (2001). The Salmonella spvB virulence gene encodes an enzyme that ADP-ribosylates actin and destabilizes the cytoskeleton of eukaryotic cells. *Molecular Microbiology*, *39*(6), 1464–1470. https://doi.org/10.1046/j.1365-2958.2001.02360.x

Luo, X., & Lee Kraus, W. (2012). On par with PARP: Cellular stress signaling through poly(ADP-ribose) and PARP-1. *Genes and Development*, *26*(5), 417–432. https://doi.org/10.1101/gad.183509.111

Palazzo, L., Mikoč, A., & Ahel, I. (2017). ADP-ribosylation: New facets of an ancient modification. *FEBS Journal*, *284*, 2932–2946. https://doi.org/10.1111/febs.14078

Pulliainen, A. T., Hytönen, J., Haataja, S., & Finne, J. (2008). Deficiency of the Rgg regulator promotes H2O2 resistance, AhpCF-mediated H2O2 decomposition, and virulence in Streptococcus pyogenes. *Journal of Bacteriology*, *190*(9), 3225–3235. https://doi.org/10.1128/JB.01843-07

Robaszkiewicz, A., Erdélyi, K., Kovács, K., Kovács, I., Bai, P., Rajnavölgyi, É., & Virág, L. (2012). Hydrogen peroxide-induced poly(ADP-ribosyl)ation regulates osteogenic differentiation-associated cell death. *Free Radical Biology and Medicine*, *53*(8), 1552–1564. https://doi.org/10.1016/j.freeradbiomed.2012.08.567

Tezcan-Merdol, D., Nyman, T., Lindberg, U., Haag, F., Koch-Nolte, F., & Rhen, M. (2001). Actin is ADP-ribosylated by the Salmonella enterica virulence-associated protein SpvB. *Molecular Microbiology*, *39*(3), 606–619. https://doi.org/10.1046/j.1365-2958.2001.02258.x

Todorova, T., Bock, F. J., & Chang, P. (2014). PARP13 regulates cellular mRNA post-

transcriptionally and functions as a pro-apoptotic factor by destabilizing TRAILR4 transcript. *Nature Communications*, *5*(1), 5362. https://doi.org/10.1038/ncomms6362

Uchida, I., Ishihara, R., Tanaka, K., Hata, E., Makino, S. I., Kanno, T., … Kubota, T. (2009). Salmonella enterica serotype Typhimurium DT104 ArtA-dependent modification of pertussis toxin-sensitive G proteins in the presence of [32P]NAD. *Microbiology*, *155*(11), 3710–3718. https://doi.org/10.1099/mic.0.028399-0

Valle, E., & Guiney, D. G. (2005). Characterization of Salmonella-induced cell death in human macrophage-like THP-1 cells. *Infection and Immunity*, *73*(5), 2835–2840. https://doi.org/10.1128/IAI.73.5.2835-2840.2005

VanEngelenburg, S. B., & Palmer, A. E. (2008). Quantification of Real-Time Salmonella Effector Type III Secretion Kinetics Reveals Differential Secretion Rates for SopE2 and SptP. *Chemistry & Biology*, *15*(6), 619–628. https://doi.org/10.1016/j.chembiol.2008.04.014

Verheugd, P., Forst, A. H., Milke, L., Herzog, N., Feijs, K. L. H., Kremmer, E., … Lüscher, B. (2013). Regulation of NF-κB signalling by the mono-ADP-ribosyltransferase ARTD10. *Nature Communications*, *4*. https://doi.org/10.1038/ncomms2672

Wei, H., & Yu, X. (2016). Functions of PARylation in DNA Damage Repair Pathways. *Genomics, Proteomics and Bioinformatics*, *14*(3), 131–139. https://doi.org/10.1016/j.gpb.2016.05.001

Welsby, I., Hutin, D., Gueydan, C., Kruys, V., Rongvaux, A., & Leo, O. (2014). PARP12, an interferon-stimulated gene involved in the control of protein translation and inflammation. *Journal of Biological Chemistry*, *289*(38), 26642–26657. https://doi.org/10.1074/jbc.M114.589515

Yang, C., Jividen, K., Spencer, A., Dworak, N., Ni, L., Oostdyk, L. T., … Paschal, B. M. (2017). Ubiquitin Modification by the E3 Ligase/ADP-Ribosyltransferase Dtx3L/Parp9. *Molecular Cell*, *66*(4), 503–516.e5. https://doi.org/10.1016/j.molcel.2017.04.028

Zhang, Y., Wang, J., Ding, M., & Yu, Y. (2013). Site-specific characterization of the Asp- and Glu-ADP-ribosylated proteome. *Nature Methods*, *10*, 981. Retrieved from https://doi.org/10.1038/nmeth.2603